CTM-BASED MACROSCOPIC TRAFFIC FLOW MODEL CALIBRATION AND VALIDATION FOR DHAKA CITY

H. M. Imran Kays

DEPARTMENT OF CIVIL ENGINEERING

MILITARY INSTITUTE OF SCIENCE AND TECHNOLOGY (MIST)

December 2016

CTM-BASED MACROSCOPIC TRAFFIC FLOW MODEL CALIBRATION AND VALIDATION FOR DHAKA CITY

H. M. Imran Kays

(BSc in Civil Engineering, MIST)

A THESIS SUBMITTED

FOR THE DEGREE OF MASTER OF SCIENCE

DEPARTMENT OF CIVIL ENGINEERING

MILITARY INSTITUTE OF SCIENCE AND TECHNOLOGY (MIST)

December 2016

The thesis titled **"CTM-Based Macroscopic Traffic Flow Model Calibration and Validation for Dhaka City"** Submitted by H. M. Imran Kays, Roll No: 1014110012 Session: 2014-15 has been accepted as satisfactory in partial fulfillment of the requirement for the degree of Masters of Science in Civil Engineering (Transportation Engineering) on 01st December 2016

BOARD OF EXAMINERS

1. _____ Chairman

Dr. Md. Hadiuzzaman (Supervisor)
Associate Professor,
Department of Civil Engineering,
Bangladesh University of Engineering and Technology, Dhaka

2. _____ Member

Col Shah Md. Muniruzzaman, psc (Ex-officio)
Head, Department of Civil Engineering
Military Institute of Science and Technology, Mirpur, Dhaka

3. _____ Member

Major Mohammed Russedul Islam, PhD, Engrs (Internal)
Instr Cl-'B',
Department of Civil Engineering
Military Institute of Science and Technology, Mirpur, Dhaka

4. _____ Member

Dr. Md. Mizanur Rahman (External)
Professor,
Department of Civil Engineering,
Bangladesh University of Engineering and Technology, Dhaka

DECLARATION

I hereby declare that this thesis is my original work and it has been written by me in its entirety. I have duly acknowledged all the sources of information which have been used in the thesis.

This thesis has also not been submitted for any degree in any university previously.

_____

H. M. Imran Kays

01 December 2016

ABSTRACT

The road network system of Dhaka city is predominantly non-lane-based and heterogeneous in nature. Although microscopic model can simulate this traffic condition, it is difficult to simulate in any macroscopic traffic flow model. The choice of macroscopic model has become very popular these days, because these models consider aggregate behaviour of a set of vehicle i.e. traffic stream as a whole. These models are not only easier to observe and validate depending upon the traffic condition and roadway environment but also demand very less parameters, which are easier to achieve from the field. The main advantage of using these models is to predict and evaluate traffic over time and space in a very short time, including transient phenomena such as the building, propagation, and dissipation of queues, which is very useful in active traffic management and traffic control strategy. Considering all these, this research develops a new modified Cell Transmission Model (CTM) for Dhaka city, a first-order macroscopic model, which can simulate non-lane-based heterogeneous traffic accurately.

The modified CTM takes the parameter values from Fundamental Diagram (FD), which has to be modelled prior to CTM. For this high-resolution data was collected from a stretch of 3.26KM roadway divided in 5 cells. Interestingly, FD is found variable in different cells. To confirm the structure of the FD, initially the speed-density plots of the field data for different links are fitted with four general structures: namely, the linear, logarithmic, exponential and polynomial forms. It is revealed that the 3rd degree polynomial structure is best suited for prevailing traffic condition. The boundary values of the experimental setup then fed into modified CTM i.e. length of each cells, free-flow speed, critical density, jam density and capacity. The non-linear equations of FD for heterogeneous traffic behaviour then incorporated in the computational algorithm to modify CTM. This new model, incorporating the new calibration methodology, simulate the traffic system of the experimental setup. The model is then validated comparing with the field data. The sensitivity analysis proves that the modified CTM can simulate the system of heterogeneous traffic with better accuracy than the original CTM.

ACKNOWLEDGEMENTS

All praise goes to almighty Allah, the most merciful and the most beneficent.

I would like to express my deepest gratitude to my supervisor and Chairmen of the Board of Examiner Dr. Md. Hadiuzzaman, Associate Professor, Department of Civil Engineering, BUET, Dhaka for his guidance, encouragement, enthusiastic directions and continuous support throughout the research work.

I also express my sincere appreciation and gratitude to the member of the Board of Examiner: Professor Dr. Md. Mizanur Rahman, Colonel Shah Md. Muruzzaman, psc, Major Mohammed Russedul Islam, PhD, Engrs for their thoughtful questions, valuable comments and suggestions.

I would like to acknowledge the research grant received for this study from the Committee for Advanced Studies and Research (CASR) of MIST, Dhaka.

I am also thankful to Sanjana Hossain, Lecturer, Department of Civil Engineering BUET, Sarder Rafee Musabbir, Graduate Research Assistant, Department of Civil Engineering and Nazmul Haque, Research Assistant, Department of Civil Engineering, BUET for his extensive support and help.

Finally and most importantly, I am grateful to my parents for their love, concern, care and faith without which this study would have been impossible.

TABLE OF CONTENTS

LIST OF TABLES

LIST OF FIGURES

CHAPTER 1

INTRODUCTION

1.1 Background of the Study

Dhaka, capital of Bangladesh, one of the biggest and densely populated city having large business activity all around. This city has 47.4 million populations in 104.2 sq. mile and population growth rate is 2.94% per year [1]. Metropolitan Chamber of Commerce and Industry (MCCI) and Chartered Institute of Logistics and Transport Bangladesh in 2010 found that the annual cost of traffic congestion in capital Dhaka was around Take 19,555cr per year, which contributes to almost 35% of total GDP. The study found that about 3.2 million business hours are lost every day, which is about one hour per working people. Dhaka city is trying to accommodate this huge traffic movement with infrastructure development, i.e. road building, fly-over, over-pass etc. However, this results in a poorly planned development and expunction of this city and the consequence is a set of complex road network. In 2012, Dhaka Metropolitan Area has approximately 3,000 km road network in which only 200 km primary road, 110 km secondary, 152 km feeder, 2640 km narrow and of then only 400 km road has footpath. In 2005 STP found from its household survey that, about one third of population use rickshaw (Non-Motorized Vehicle- NMV) of about 34%, interested to walk 14%, use transit 44% and only 8% use motorized non-transit type modes[1] of total trip distribution. On the other hand, public transports especially buses access only on 2.5% of the total road network includes only 11.5% of total traffic but carry about 77% of people [2]. Since the population comprises diversified class of people, land use pattern and use of transport facilities differ greatly. This diversity causes the heterogeneous traffic nature in this city.

1 Non-Transit includes car, van, pickup, auto-rickshaw, taxi and motorcycle

The lane discipline is also not maintained in traffic network of Dhaka city. The main reason behind this are the heterogeneity of traffic system with different speed class vehicle and absence of dedicated lane for specific vehicle. Though the slow moving heavy vehicles[2] has restriction to enter the city before 2000hrs, the inter-city NMV, public buses, pickups etc. reduces the speed of the whole network. This results in a competition of speed followed by overtaking tendency among drivers. Moreover, congestion at consecutive intersection makes the situation more agitated. The outcome is non-lane-based traffic behaviour. There are some other factors that affect this behaviour, like presence of roadside friction comes from roadside market, presence of footpath, On- and Off-Ramp, pedestrian activity etc. Another major cause of non-lane-base behaviour comes from geometry of the roadway network i.e. presence of bus-bay in improper location, which also results in weaving, dropping of speed and hence reduce capacity.

This nature of traffic stream made it difficult to establish a standard traffic flow model followed in developing countries with homogeneous and lane disciplined traffic. As a result, it has become essential to develop a calibrated and validated macro-model, which consider the traffic stream's aggregate behaviour, can even simulate traffic flow more accurately. This in turn will assist city transport planners to investigate impact of different traffic control and management strategies before field deployment.

Cell Transmission Model (CTM) [3] is a widely used dynamic macroscopic traffic flow model which is used to evaluate traffic movement over time and space. Moreover, this model can be implemented to investigate queue development, propagation and dissipation under congested traffic condition. This model consider the whole network and divide it into small cells. With this consideration the model can

2 Heavy Vehicle includes Truck, Trailer, Covered Van, Lorry etc.

predict spillback and dissipation of queue in a reasonable and dynamic way [3]. This model is consistent with the state-of-the-art kinematic wave theory proposed by Lighthill, Whitham and later Richards (LWR) [4]. This model uses traffic demand profile, density dynamics and fundamental diagram (FD) parameters to simulate flow; however, cannot predict dynamic route choice. FD represents empirical relationship between speed-flow-density, is the centrepiece to macroscopic flow model to evaluate link specific free-flow and congestion region, capture critical density, jam density, shockwave, queue size and journey time [5, 6].

1.2 Statement of the Problem and Opportunities

1.2.1 Absence of Appropriate High-Resolution Data Collection Technique

Within the vast literature on macroscopic traffic flow modelling, surprisingly very few studies have addressed the heterogeneous traffic condition, predominant in many developing countries like Bangladesh, India etc. Such limited research is primarily attributed to the difficulty of high-resolution data collection in the stated traffic condition. Here loop detectors are not suitable due to measurement errors caused by non-lane-based movement of vehicles, which will activate either both or neither of two adjacent detectors. Moreover, traffic cameras for vehicle detection and management purpose are absent along the corridors. But accurate high-resolution traffic data is the pre-requisite for developing a successful traffic flow model. This research attempts to establish a data collection technique based on image processing which will be able to measure traffic states in the non-lane-based heterogeneous operating condition with reasonable accuracy. In addition, the developed technique is expected to be robust and easy-to-use.

1.2.2 Unobserved Nature of Fundamental Diagram

Although the conservation equation used in the macroscopic models is an exact equation, the description of average speed is essentially empirical in nature and derived based on a static flow-density or speed-density relationship i.e. the Fundamental Diagram (FD). It is generally recognized that FD is dependent on flow conditions and roadway environments. Consequently, various structures of the FD have already been adopted in different models to capture the functional relationship for the whole range of traffic situations; from free flow to congested equilibrium states including non-equilibrium transitions between them. For instance, the FD corresponding to the flow-density relationship in the basic CTM was considered as trapezoidal shaped, but further adapted as continuous, piecewise differentiable FDs, such as a triangular FD. The METANET considers an exponential speed-density relationship, which is later extended to explain the impact of the VSL, ramp metering etc. on traffic flow. These structures of the FD are found to reproduce the relevant traffic conditions for homogeneous traffic scenario with remarkable accuracy. However, due to different microscopic characteristics of vehicles in heterogeneous traffic compared to the homogenous condition, the aggregated macroscopic behaviour is likely to be different. This necessitates extensive investigation of FD structures for understanding flow transition phenomenon under the non-lane-based heterogeneous traffic conditions. Unfortunately, very few field studies have been undertaken for this investigation and so there remains much scope of research in this area.

1.2.3 Absence of Appropriate Macroscopic CTM for Heterogeneous Non-Lane-Based Traffic

Among various applications of macroscopic traffic models, dynamic traffic state estimation is one of the major field of implication. The accuracy of traffic state

estimation and prediction affect the strategy for mitigating the congestion and other traffic operation related problems. Unfortunately, no such macroscopic first order discrete model has yet been developed for simulating the non-lane-based heterogeneous traffic condition, prevailing in Dhaka city. Hence, as a stepping-stone for Active Traffic Management (ATM) implementation, an appropriate macroscopic model has to be developed for the stated traffic condition by proposing necessary modifications to state-of-the-art traffic flow models. The modified model should be able to reproduce the wide variation in operating conditions and performance characteristics of vehicles in heterogeneous traffic systems successfully. More specifically, it should be able to capture the rapid change of traffic states along the roadway in that condition. Previous studies shows that all variants of the basic CTM can capture specific vehicle classes (e.g., truck, car) but cannot capture heterogeneity of mixed vehicle class, the essence of which is critical to many applications in practice [7]. As a result, considerable prediction errors exist between the measured data and the model-predicted traffic states in such operating condition. Moreover, there remains some inherent differences between lane-based and non-lane based operations which affect the overall mobility of the traffic stream. Therefore, these problems need be investigated thoroughly to improve the sensitivity of the model field performance and applicability under various traffic conditions.

1.3 Research Objectives and Scope of Work

Considering the above situation, this thesis work mainly aims at developing CTM-based macroscopic traffic flow model to simulate and evaluate traffic conditions under non-lane-based heterogeneous operating condition. With this end in view, the main objectives of the study are listed below:

- To develop a CTM-based macroscopic model for urban road network of Bangladesh.

- To calibrate and validate the model which is capable of estimating and predicting traffic states accurately for heterogeneous traffic system.

The scope of this research is limited to uninterrupted arterials (including on-ramps and off-ramps) having heterogeneous motorized traffic. The test site is the Tongi Diversion Road, a section of the Dhaka-Mymensingh Highway (N3) in Bangladesh (Figure 1.1). It is an 8-lane major artery road in Dhaka, which connects the capital city with the Shahjalal International Airport and other suburban cities. The developed model is expected to estimate and predict the complex nature of the prevailing heterogeneous traffic condition of the test site accurately through appropriate modifications and extensions of conventional traffic models.

Although arterial roads with signal controls are not included in the study, the methodological calibration used in this research can be extended and applied to other types of roadways. The research is carried out using both simulations and field data obtained from the studied roadway section. The main test site is illustrated in Figure 1.1.

1.4 Organization of the Thesis

This thesis consisting of five chapters are structured as follows:

Chapter 1 gives an introduction of the relevant research background, statement of problems as well as the objectives and scope of this research.

Chapter 2 comprehensively reviews previous works on traffic flow models with a special focus on microscopic car-following models as well as first-order and second-order macroscopic models. The traffic models are reviewed with respect to their categories in terms of *level of detail*, *scale of independent variables* and *nature of independent variables*.

Chapter 3 presents details of the study site selected and the high-resolution data collection and processing techniques adopted for the research. Some justifications regarding the choice of the methods employed are also provided.

Chapter 4 proposes a modified CTM macroscopic model for the heterogeneous traffic condition of Dhaka city. For this, at first the basic computational algorithm of CTM is discussed. Then the nature of the traffic flow and the structures of the FD of different links of the study section utilizing the collected field data are investigated, hence the most appropriate characteristic FD is modelled and is selected for our simulation. Shockwave equations are also been derived from the modelled FD. Based on the results of this investigation and other empirical observations, the dynamics of the proposed model are described. Then the algorithm of the proposed model is discussed along with the mathematical expressions. Then the developed model is calibrated from FD and validated using field data of another day to test its performance. Finally, the sensitivity of the model and field applicability in other links of similar traffic scenario are discussed.

Chapter 5 summarizes the main conclusions of this research and discusses recommendations for future research works related to macroscopic traffic flow models and simulation for heterogeneous traffic.

Figure 1.1 The 3.26 km long study site between Armed Forces Medical College and CAAB Head Quarters (courtesy: Google maps). Details can be found in Figure 3.1.

CHAPTER 2

LITERATURE REVIEW

Traffic flow theory, describing traffic engineering was considered as a practical discipline, involving most of the time a common sense of its practitioners to solve particular traffic problems in its initial stage. However, this has changed at the dawn of the 1950s, when the scientific field began to mature, attracting engineers from all sorts of fields. Most notably, John Glen Wardrop [8] instigated the evolving discipline, traffic flow theory, by describing traffic flows using mathematical and statistical ideas. During this highly active period, mathematics established itself as a solid basis for theoretical analyses, a phenomenon that was entirely new to the previous development. This gives this 'common sense' – a mathematical validation for establishing the theory. Two examples of the progress during this decade, include the fluid-dynamic model of Lighthill, Whitham and Richards (LWR) for describing traffic flows [4], and the car-following experiments and theories of the club of people working at General Motors' (GM) research laboratory [9]. Again, to correlate freeway speed, density and flow Greenshields in 1934 made a breakthrough by developing fundamental diagram [6]. He used photographic images to estimate aggregate vehicular speeds and densities on a straight two-lane roadway, and found that they could reasonably be well approximated by a straight line like in figure 2.1. Using figure like 2.1, he later developed parabolic relationship between flow and density.

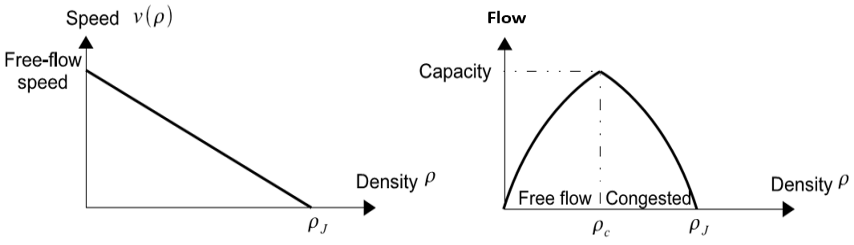

Figure 2.1 Greenshild's speed, density and flow relations.

Since then, numerous modelling approaches has been developed, from simple one-regime linear speed-density relationships to multi-regime, multi-class, nonlinear models. This chapter presents a historical overview of a rich variety of modelling approaches developed so far and in use today. Here, theoretical issues of model derivation and characteristics and some practical issues, such as model calibration and validation will also be discussed.

2.1 The Quantitative Terms

The Highway Capacity Manual 2000 [10] provides the following definitions of the basic quantities. Symbols *x* and *t* represent position (measured in the direction of traffic flow) and time respectively.

a. **Speed *v(x,t)*** is a rate of motion expressed as distance per unit of time. Depending on how it is measured, it is referred to as either space mean speed or time mean speed. Space mean speed is computed by dividing the length of a road by the average time it takes for vehicles to traverse it. Time mean speed is the average speed of vehicles observed passing a given point.

b. Free flow speed v_f is the average speed of traffic measured under conditions of low volume, when vehicles can move freely at their desired speed.

c. Flow q(x,t) is the total number of vehicles that pass by the point x during a given time interval t , divided by the length of the time interval t.

d. Density ρ(x,t) is the numb er of vehicles occupying a length of road about point x at time instant t . Its measurement is difficult because it requires the observation of a stretch of road. Instead, it is often approximated from measurements of flow and speed as:

$$\rho(x,t) = \frac{q(x,t)}{v(x,t)} \quad \text{---------- 2.1}$$

e. **Demand** is the number of vehicles that desire to use a given facility during a specified time.

f. **Capacity** is the maximal hourly rate at which vehicles reasonably can be expected to traverse a point or a uniform section of a lane or roadway during given time period under prevailing roadway, traffic and control conditions.

g. **Bottleneck** is defined as any road element where demand exceeds capacity. Freeway bottlenecks sometimes appear near heavy on-ramps, where a localized increase in demand is combined with a decrease in capacity due to lane changing.

2.2 Categorizations of Traffic Flow Models

Traffic flow models can be categorized according to various criterion, such as the *level of detail represented* in the model, *the scale of independent variables, the nature of variables used in modelling, operationalization criterion of the models, their scale of application* etc. These classes are discussed briefly in the following sub-sections.

2.2.1 Level of Detail

The scope of traffic flow models can be differentiated either by considering the time-space behaviour of individual drivers under the influence of vehicles in their behaviour (microscopic models), the behaviour of drivers without explicitly distinguishing their time-space behaviour (mesoscopic models), or from the viewpoint of the collective vehicular flow (macroscopic models). Broadly, these models can be classified into four categories according to the level of detail with which they represent the traffic systems. These are:

a. Sub-Microscopic Models

These are highly detailed descriptions of the functioning of vehicle motions, where even the behaviour of specific vehicles sub-units and the interaction with their

surroundings are considered. From the driver's point of view, there are three main actions that directly influence traffic flow dynamics: Accelerating, braking, and steering. These actions are part of the vehicle dynamics and therefore can be included in the domain of sub-microscopic models. Traffic flow dynamics in these models describes the dynamics one level higher than microscopic models by directly modelling lane-changing decisions and the associated actions.

b. Microscopic Models

These models take each individual vehicle as a unit and track its motion and interaction with adjacent vehicles in the traffic stream. They operate based on the properties of each vehicle and on a set of rules. Typical examples of this kind of model are the *car-following models* for longitudinal movement and the *lane changing models* for lateral movement on multi-lane roadways, on-ramps and off-ramps.

c. Mesoscopic Models

These are medium-detailed models where small groups of interacting vehicles are traced, instead of individual vehicle units. These models combine microscopic and macroscopic approaches to a hybrid model, use parameters of a microscopic model which otherwise depend on macroscopic quantities such as traffic density or local speed and speed variance. Conversely, the dynamics of a macroscopic quantity like the number of vehicles in a traffic jam is described in terms of microscopic stochastic rate equations for in- and out-flowing vehicles.

d. Macroscopic Models

These models are low-detailed representations of traffic states using aggregated variables, such as flow, average speed and density. They describe the collective effect of many vehicles. Individual vehicle motions and interactions are completely neglected. These models are often derived from the analogy between vehicular flow and the flow

of continuous media (e.g. fluids or gases). Detailed description of sub-microscopic and mesoscopic models are not included hereafter, since they are out of the scope of this research. However, a comprehensive review on all these types of traffic flow models can be found in Hoogendoorn and Bovy [8].

2.2.2 Scale of the Independent Variables

According to the scale of independent variables, traffic flow models can be classified as either continuous models or discrete models.

a. Continuous Models

The independent variables of these models change continuously and instantaneously both in time and space in response to continuous stimuli. These models are often formulated as differential equations in which time and space are treated as continuous variables over the study domain. Most of the car-following models are examples of this approach and so are hydro-dynamic macroscopic models.

b. Discrete Models

These models assume discontinuous changes in both time and space. Accordingly, traffic states are described temporally and spatially at discrete steps along the roadway. Examples of such discrete models include the cellular automata model (CA), the Cell Transmission Model (CTM) etc.

2.2.3 Nature of the Independent Variables

According to the nature of independent variables used for representing the operation processes, traffic flow models can be distinguished as deterministic and stochastic models.

a. Deterministic Models

In these models, all the factors are defined by exact relationships, i.e. there are no randomized components of these models. Random elements can be used to describe aspects of the traffic flow, which are unknown, immeasurable, impossible to model, or "genuinely" random. While models without any randomness are called deterministic models. In discrete models, if a traffic situation is simulated twice using a deterministic model, starting from the same initial conditions and with the same inputs and boundary conditions, the outputs of both simulations always remain same. The Cell Transmission Model, METANET model are examples of a deterministic traffic model.

b. Stochastic Models

Stochastic model descriptions use random variables (known as noise terms or stochastic terms like acceleration noise, exogenous noise, parameter noise and heterogeneities) and a probabilistic approach to describe traffic states. This implies that two simulations of the same model starting from the same initial conditions, the same boundary conditions and the same inputs may return different results, depending on the value of the stochastic variable during each simulation. A stochastic variable can be characterized by its distribution function or by its histogram. For example, in the microscopic simulation package Paramics, a distribution of the level of patience over different drivers needs to be defined. During simulation, this distribution is sampled to determine an individual level of patience for every driver simulated in the network. A second simulation, and thus a new sampling of the distribution, will result in drivers with other levels of patience. Therefore, stochastic models need to be simulated repeatedly and the results need to be averaged in order to be able to draw conclusions. Stochastic variables are used to model stochastic processes present in real-life traffic situations.

2.3 Microscopic Traffic Flow Models

As mentioned earlier, microscopic traffic models describe the space–time behaviour of the system's entities (i.e. vehicles and drivers) as well as their interactions at a high level of detail (individually). In other words, these models simulate the longitudinal (car following) and lateral (lane-changing) behaviour of individual vehicles in relation to the roadway and other vehicles in the traffic flow. From this point of view, the microscopic traffic flow models are broadly classified into two categories: (i) *the car following* and (ii) *the lane-changing models*. Both of these types are reviewed in detail in the following sub-sections.

Table 2.1 Delimitation of traffic flow dynamics from vehicular dynamics and transportation planning

Time scale	Field	Models	Aspect of traffic (examples)
<0.1 s	Vehicle dynamics	Sub-microscopic	Control of engine and brakes
1 s			Reaction time, time gap
10 s	Traffic flow dynamics	Car-following models	Acceleration and deceleration
1 min		Macroscopic models	Cycle period of traffic lights
10 min			Stop-and-go waves
1 h			Peak hour
1 day		Route assignment traffic demand	Daily demand pattern
1 year	Transportation planning		Building/changing infrastructure
5 years		Statistics age pyramid	Socioeconomic structure
50 years			Demographic change

2.3.1 The Car-Following Models.

In the car-following theory, the relation between the preceding vehicle and the following vehicle is described that each individual vehicle always decelerates or accelerates as a response of its surrounding stimulus. Therefore, the n^{th} vehicle's motion equation can be summarized as follows:

$$[response]_n \propto [stimulus]_n \quad \text{---------- (2.2)}$$

The types of the model vary according to the definitions of the stimulus. However, generally speaking, the stimulus may include the velocity of the vehicle, the acceleration of the vehicle, the relative velocity and spacing between the n^{th} and $(n+1)^{th}$ vehicle where the n^{th} vehicle follows the $(n+1)^{th}$ vehicle.

Research efforts were focused on the development of such follow-the-leader models from the 1960s when Pipes [11] proposed an expression for the position of the leader vehicle as a function of the position of its follower. Three categories of car-following models will be briefly reviewed here, namely *safe-distance models*, *stimulus-response models* and *psycho-spacing models*. Other types of car-following models include the *intelligent driver models*, *optimum velocity models*, *fuzzy logic-based models* etc. Extensive reviews of different types of car-following models can be found in established literatures like Brackstone and McDonald [12] and Wilson and Ward [13].

2.3.1.1 Safe-Distance Models

In safe-distance or collision avoidance models, the driver of the following vehicle is assumed to always keep a safe distance from the vehicle in front, so that a collision will never happen. The first and the simplest model of this category was given by Pipes [11], where the minimum safe distance between the leader and the following vehicle was assumed to be a function of the speed of the following vehicle (in miles per hour [mph]) and the length of the vehicle (in feet) in front, as indicated in Equation 2.3.

$$D_v(v) = L_n\left(1 + \frac{v}{1.47 \times 10}\right) \quad \text{---------- (2.3)}$$

Here, $D_n(v)$ is the gross distance headway of the following vehicle driving with n driving with v with respect to the leading vehicle (n-1) that must be maintained to avoid collision between them. L_n denotes the length of vehicle n and 1.47 is a conversion

factor to convert from mph to ft/s. Thus, Pipes model is a simple linear car-following model, which essentially states that that the minimum safe distance between two vehicles. This model assumed that the minimal time headway was equal to the class-specification reaction time and the time required for the vehicle to travel a distance equal to its length.

Kometani and Sasaki [12] derived a car-following model from basic Newtonian equations of motion. They sought to specify a safe following distance within which a collision would be unavoidable, if the driver of the vehicle in front were to act 'unpredictably'. This model is a nonlinear regression model with parameters related to the speed of the pair of vehicles.

Gipps [14] refined safe-distance car-following models by assuming that the driver travels as fast as safety and the limitations of the vehicle permit:

$$v_n(t+\tau) = \min \left\{ \begin{array}{l} v_n(t) + 2.5 a_{\max} \tau \left(1 - \frac{v_n(t)}{v_{\max}}\right) \sqrt{0.25 - \frac{v_n(t)}{v_{\max}}}, \\ a_{\min} \tau + \sqrt{\left(a_{\min}{}^2 \tau^2 - a_{\min} \left(2(x_{n-1}(t) - x_n(t) - s_{jam}) - v_n(t)\tau - \frac{v^2{}_{n-1}(t)}{b} \right)\right.} \end{array} \right\} \text{---- (2.4)}$$

Where a_{max} maximum acceleration, a_{min} maximum deceleration (minimum acceleration), v_{max} the desired (maximum) velocity and s_{jam} jam spacing. s_{jam} is the jam spacing which is the front-to-front distance between two vehicles at standstill. Effectively, Gipps' [14] approach introduced two regimes: one in which the vehicle itself limits its velocity [the top part in Equation 2.4], and one in which the safe distance to the leader limits velocity (the bottom part in the Equation 2.4).

Leutzbach [15] discussed a more refined model describing the spacing of constrained vehicles in the traffic flow. He states that the overall reaction time T consists of:

a) Perception time (time needed by the driver to recognize that there is an obstacle),

b) Decision time (time needed to make a decision to decelerate) and

c) Braking time (time needed to apply the brakes).

The safety distance model assumes that drivers consider braking distances large enough to permit them to brake to a stop without causing a rear-end collision with the preceding vehicles if the latter vehicles come to a stop instantaneously.

2.3.1.2 Stimulus-response Models

The second branch of car-following models discussed in this research consists of stimulus–response models. The car-following process of these models is based on the following basic principle:

Response (t+τ) = Sensitivity x Stimulus (t) ---------- (2.5)

A stimulus at time *t* together with the driver's sensitivity causes a driver reaction after a reaction time τ. The stimulus is usually represented by the relative velocity (speed difference) of the leading and the following vehicle or the spacing between the two vehicles. The response is represented by the acceleration or deceleration of the following vehicle.

During the late 1950s and early 1960s there was a rapid development of the stimulus-response models. The first model of this category was proposed by Chandler et al. [16]. They assumed that the sensitivity term was a constant and the response was in the form of:

$$a_n(t+\tau) = \gamma[v_{n-1}(t) - v_n(t)] \quad \text{---------- (2.6)}$$

Where, $v_n(t)$ and $a_n(t)$ denote velocity and acceleration respectively of vehicle n at t and γ is the sensitivity of the following vehicle that needs to be determined in experiments or model calibration. This model is a linear model with speed difference as the stimulus.

Subsequent researches on stimulus-response models were aimed at improving the description of the sensitivity of the following vehicle. These are included using different sensitivity factors for acceleration and deceleration [17], introducing the distance between two vehicles and the speed of the following vehicle.

All these efforts behind improving the stimulus-response models are consolidated in the now famous Gazis-Herman-Rothery (GHR) model [18], named after Gazis et al. This model considers exponents of both speed and distance in the sensitivity term thus improving the overall accuracy of the model.

$$a_n(t+\tau) = \frac{\alpha_{1,m}[v_n(t+\tau)]^m}{[x_{n-1}(t) - x_n(t)]^l}[v_{n-1}(t) - v_n(t)] \quad \text{---------- (2.7)}$$

Where, x_{n-1} and v_{n-1} represent position and speed of the leading vehicle, respectively, and x_n, v_n and a_n represent position, speed and acceleration of the following vehicle, respectively. m is the speed exponent, l is the distance headway exponent and $\alpha_{1,m}$ is a model constant. By assuming different values of m and l, several special cases of car-following models can be obtained.

However, the GHR model simulates the behaviour of free-flowing drivers very unrealistically. For example, the model assumes that the follower reacts to the actions of the leader, even though the distance to the leader is very large, and that the follower's response disappears as soon as the relative speed is zero. In addition, according to the model, slow drivers are dragged along when following faster vehicles. This is obviously different from real-world traffic. These shortcomings can be corrected by either extending the GHR-model with additional regimes, e.g., free driving, emergency deceleration, etc., or by using a *psycho-physical* model or *fuzzy logic-based models*. Some of the most popular more recent stimulus–response models include the optimal velocity model with delay by Bando et al. [19], the two-regime intelligent driver model

by Treiber et al. [20], the acceleration delay model by Kerner and Klenov [21], the stochastic car-following model by Kerner and Klenov [22] etc.

2.3.1.3 Psycho-Spacing Models

This approach to car-following modelling is based on behavioural thresholds referred to as action points and was first proposed by Michaels [23]. It remedies the problems of stimulus-response models identified in the previous section by using insights from perceptual driver psychology. The idea is that drivers are subject to certain limits in their perception of the stimuli to which they respond. It is thus possible to identify space-time thresholds that trigger different acceleration profile characterizations of a driver. Drivers will react to changes in speed difference or spacing only when these thresholds are reached [15]. The basic behavioural rules of such so-called psycho-spacing models are:

a. At large spacings, the following driver is not influenced by velocity differences.
b. At small spacings, some combinations of relative velocities and distance headways do not yield a response of the following driver, because the relative motion is too small.

The most famous psycho-spacing model was developed by Wiedemann [24]. He distinguished constrained and unconstrained driving by considering perception thresholds. This car-following model utilizes these perception thresholds to describe the longitudinal motion of individual vehicles. The main concept of the model is that the follower starts to adjust its speed by applying continuous deceleration as it reaches its own perception threshold to a slower lead vehicle. However, since it cannot exactly determine the speed of the lead vehicle, the follower's speed will drop below the lead vehicle's speed until the follower applies slight acceleration after reaching another

perception threshold. This results in an iterative process of acceleration and deceleration.

There are four different stages of following a lead vehicle:

a. **Free driving**: In this mode, there is no influence of the lead vehicle. The follower travels at its desired speed.
b. **Approaching**: In this mode, the follower tries to adapt to the lead vehicle's speed. The follower applies a continuous deceleration so that the speed difference between them is zero when it reaches its desired safety distance.
c. **Following**: In this mode, two close vehicles maintain a safe distance, and their relative speed fluctuates around zero. The follower maintains its speed close to the lead vehicle without any conscious acceleration or deceleration.
d. **Braking**: In this mode, the relative distance between vehicles falls below a safe distance. This could be a result of a sudden deceleration of the lead vehicle; a third vehicle merges in front of the follower, etc.

Other noteworthy psycho-spacing models include the models of Lee & Jones [25] [which uses spacing-based threshold for driver perception], Evans and Rothery [26] [which quantifies Michaels' [23] thresholds through a series of perception-based experiments], Krauss et al. [27] [which addresses transient traffic flow behaviour, like the capacity drop, and stability of so-called wide jams] etc.

Psycho-spacing models are the foundation of a number of contemporary microscopic simulation models. For example, the microscopic simulation package, VISSIM (PTV 2012) which is described in detail in Chapter 5, uses the psycho-physical driver behaviour model proposed by Wiedemann [24].

2.3.2 Lane-Changing Models

Lane changing refers to the lateral movements of vehicles from one lane to another. It may happen mandatorily at merge and diverge areas, or voluntarily at multi-lane roadways. Near on-ramp or lane-drop areas, merging manoeuvres are one of the direct causes for the overloading of certain lanes and may lead to traffic breakdown [28]. In addition, voluntary lane changing can be the origin of perturbations that may lead to jams in dense and unstable traffic. As such, most models classify lane changes as either mandatory or discretionary lane change. Although lane-changing models are not as widely studied as car-following models, it is essential to incorporate this mechanism in traffic flow models. Extensive review on lane-changing models can be found in Moridpour et al. [29].

Moridpour et al. [29] classified the different approaches taken in lane changing studies from the point of view of either driving assistance or driving decision systems. They defined driving assistance models as the models which consider the steering wheel angle and lateral motions to control the lane changing performance of vehicles. They further subdivided this category into collision prevention models and automation models. Collision prevention lane changing models are developed to control drivers' lane changing manoeuvres and assist them to execute a safe lane change. The collision prevention models are intended to improve road safety.

Moridpour et al. [29] mention the other category of lane changing models focuses on driver's lane changing decisions under different traffic conditions and under different situational and environmental characteristics. They classified driver's decisions while responding to the surrounding environment, as either strategic, tactical or operational [30]. This classification is based on the time required for executing the decisions. The strategic level is the highest decision level and deals with driver's

decisions which require over 30 seconds making and executing. While executing the strategic level decisions, a series of tactical decisions are made by the drivers, such as a decision to pass a slow moving vehicle or maintaining the desired speed. At the tactical, or intermediate, decision level, the time required for making and executing the decisions is between 5 and 30 seconds [31]. At the lowest decision level or the operational level, drivers decide about the manoeuvres to control their vehicles. These take place on a time scale of less than five seconds and include decisions such as whether or not to accept a gap [31].

A famous lane-change model is the one by Wiedemann [24], the principle of which is that drivers try to avoid discomfort in their own lane (for example, the vehicle in front is too slow compared with their desired speed) and seek the speed advantage of other lanes. This desire for lane change leads to a lane change manoeuvre, if the gap in the target lane is sufficient to perform a safe manoeuvre.

Different from car-following, in the lane-changing model, the driver's behaviour in the presence of interacting vehicular flows cannot be described as a function of the state of the leading vehicle, but must also take into account the distance and speed of the back and front vehicles on the target lane. Considering lane changing in microscopic models allows for the realization of necessary (mandatory) lane changes at on-ramps or lane closures as well as discretionary lane changes in preparation for passing slower vehicles.

2.3.3 Commercial Microscopic Simulation Models

With the increased availability of fast computers in recent years, the application of microscopic simulation as a tool to reflect real-world traffic systems is gaining popularity. The number of traffic simulation models has increased significantly and by

the end of the last century, there were more than 70 simulation models available according a study by U.C. Berkley [32]. Among the large amount of traffic simulation models, five well-known models are the CORSIM, the AIMSUN, the VISSIM, the PARAMICS, and the INTEGRATION microscopic traffic simulation models. Each traffic simulation model has its unique underlying logic. The car-following and lane-changing logics used in each of these five models are listed in Table 2.2 below.

Table 2.2 Car-following and lane-changing logics of different microscopic simulation

Microscopic Traffic Simulation Software	Car-following logic	Lane-changing logic
AIMSUN (Advanced Interactive Microscopic Simulator for Urban and NonUrban Networks)	Gipps (1981) safety-distance model	Gipps (1986) lane-changing model
PARAMICS	Psycho-physical model of Fritzche (1994)	Gap-acceptance model
CORSIM (CORidor SIMulation)	NETSIM for arterials with at-grade intersection and FRESIM for uninterrupted facilities.	Gipps (1986) lane-changing model which considers both mandatory and discretionary lane changes
INTEGRATION	Car-following models of Van Aerde (1995) and Van Aerde & Rakha (1995)	Considers both mandatory and discretionary lane changes
VISSIM	Psycho-physical models of Wiedemann (1974) for urban traffic and Wiedemann (1999) for motorway	Lane-changing model of Willmann and Sparmann (1978)

2.4 Macroscopic Traffic Flow Models

Macroscopic models are the aggregation of individual vehicle dynamics and mainly focus on describing the overall stream features such as congestion, delay, and queue formation. These models are suited for large scale, network wide applications where the macro-characteristics of traffic are of prime interest. This approach of traffic flow modelling represents the traffic states with the help of aggregated variables (*Speed, Flow and Density*) and yields flow models with a limited number of equations. Usually, these models are derived from the analogy between vehicular flow and flow of continuous media (e.g. fluids or gasses).

Two basic equations always hold in all of the macroscopic traffic flow models. One is the conservation equation, which states that the change in number of vehicles on the roadway segment (x, $x + dx$) during time interval (t, $t+dt$) is equal to the number of vehicles flowing into that segment minus the number of vehicles flowing out of that segment. That is, vehicles are neither automatically generated nor taken away on an enclosed section of roadway. This is expressed as a partial differential equation [33]:

$$\frac{\partial p}{\partial t}+\frac{\partial q}{\partial x}=g(x,t) \quad \text{---------- (2.8)}$$

Or as in an integration form:

$$\frac{\partial}{\partial t}\int_{x_1}^{x_2}\rho(x,t)dx=q(x_1,t)-q(x_2,t)+g(x,t) \quad \text{---------- (2.9)}$$

Where, q stands for flow, ρ for density and v for space-mean-speed. g is the generation rate within the road segment (from on-ramps and off-ramps), x and t stands for space and time, respectively.

Another equation is the basic traffic flow equation, namely, flow equals to the density times the space-mean-speed.

$$q=v\rho \quad \text{---------- (2.10)}$$

Equations (2.8) and (2.10) form a system of two independent equations with three unknown variables ρ, v and q. To solve this system, another independent equation is required. The different formulations of the third equation resulted in a series of macroscopic models. In this section, we discuss the two major types of macroscopic traffic models, namely, the first-order traffic models and the second-order traffic models.

2.4.1 First-Order Macroscopic Traffic Models

2.4.1.1 LWR Model

The most widely used first-order macroscopic traffic model was developed by Lighthill and Whitham and Richards (LWR model) [4, 34], which is a continuous macroscopic representation of traffic variables. In the LWR model, the speed and/or flow rate are considered as a function of density:

$$v(x,t) = V_e[\rho(x,t)] \quad \text{---------- (2.11)}$$

Hence,

$$q(x,t) = q_e[\rho(x,t)] = \rho(x,t)V_e[\rho(x,t)] \quad \text{---------- (2.12)}$$

Where, V_e denotes the equilibrium speed. It is a monotonically decreasing function of density. The relationship between density $\rho(x, t)$ and flow $q(x, t)$ is called the Fundamental Diagram (FD). The flow function is convex with a downward concavity [35]. Since Equation 2.12 does not specify the functional form of the FD, many specific functions have been proposed either from fitting the measured data or from analytical deliberations, or a combination of both.

The solution of the nonlinear Equations 2.11 and 2.12 is of the general form as in Equation 2.13 [36], which means that all points are on a straight line with slope v having the same density:

$$\rho(x,t) = F(x - vt) \quad \text{---------- (2.13)}$$

Where, F is an arbitrary function. Equation 2.13 implies that inhomogeneity, such as changes in density of vehicles, propagates along a stream of traffic at a constant speed $V_w = \partial q/\partial \rho$, which is positive or negative with respect to a stationary observer, depending on whether the density is below or above the optimum density corresponding

to maximum q (Figure 2.2). The shockwave speed is expressed in Equation (2.14) and shown in Figure 2.2.

$$V_w = \frac{q_b - q_a}{\rho_b - \rho_a} \quad \text{---------- (2.14)}$$

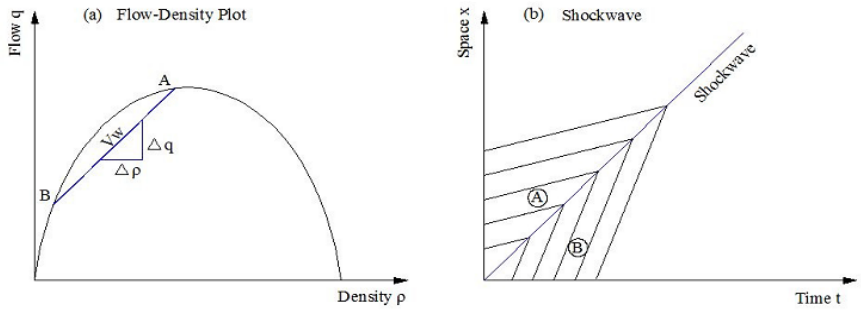

Figure 2.2 Shock wave formations resulting from the solution of the conservation.

Though the model can represent explicitly the formation of shockwaves, it is not capable of explaining other phenomena such as steady state speed–density relationship, discontinuities in the density, regular start–stop waves, traffic hysteresis, localized clusters and phantom jams.

2.4.1.2 The Cell Transmission Model

Most of the first-order macroscopic traffic flow models are discretized derivatives or extensions of the LWR model. Within this category, the Cell Transmission Model [3] is the most popular, owing to its analytical simplicity and ability to reproduce congestion wave propagation dynamics.

When simulating LWR model, outflow is typically specified as a function of occupancy of the section from which it is emitted and not as a function of downstream occupancy. Such approach does not converge to a desired solution and cannot produce reasonable results. Ensuring cell occupancies between zero and the maximum possible do not guarantee convergence, for example, stopped traffic is predicted not to flow into an empty freeway. These issues are resolved when Daganzo [3, 37] formulated a Cell

Transmission Model (CTM) as a discretization of first order LWR model. The model divides the freeway stretch into cells and uses a piecewise linear relationship between traffic flow and traffic density (triangular fundamental diagram).

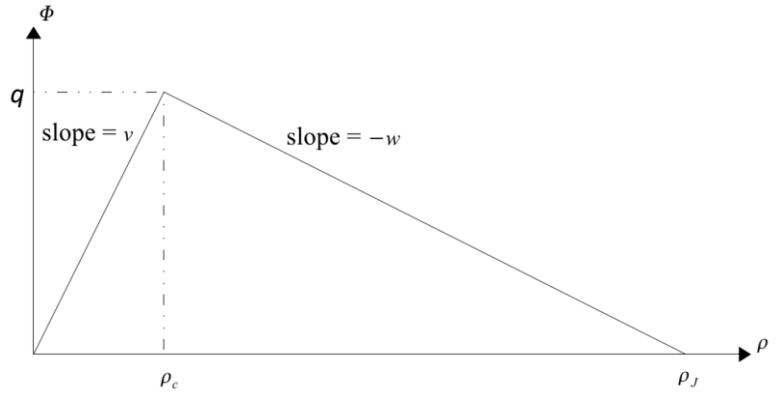

Figure 2.3 The fundamental diagram for CTM, characterized by the maximum flow (Capacity) q, Speeds v, Shockwave w, Critical Density ρ_c and Jam Density ρ_j.

In the model formulation, given a time step, the length of the cells is chosen such that under free flow conditions, all vehicles in a cell will flow into the immediate downstream cell. The model functions based on the law of vehicle conservation: the number of vehicles in cell i at the next time step (k+1) equals to the number of vehicles currently in cell i, plus the inflow from the upstream cell (i-1) to cell i and minus the outflow to the downstream from cell i to cell (i+1) between the time indexes t and (t+1). That is:

$$n_i(t+1) = n_i(t) + y_{i-1}(t) + r_i(t) - y_i(t) - s_i(t) \quad \text{---------- (2.15)}$$

Where, *i* is the cell index and t is the time index. $n_i(t)$ is the number of vehicles in cell *i* at time index t. $y_i(t)$ is the number of vehicles flowing out from cell *i*. $r_i(t)$ is the number of vehicles flowing into cell *i* from the on-ramp. $s_i(t)$ is the number of vehicles flowing out from cell *i* at the off-ramp.

The density is estimated with the following functions:

$$\rho_i(t+1) = \rho_i(t) + \frac{\Delta t}{\Delta x_i}(q_{i-1}(t) - q_i(t)) \quad \text{---------- (2.16)}$$

Where, ρ= density, q= flow, Δt= time step and Δx= length of the cell.

The number of vehicles from one cell advancing to the next cell is controlled by boundary conditions, which guarantee the number of vehicles that can flow to downstream cells. CTM has three boundary conditions: at the upstream of the first cell, an adequate number of vehicles can flow into the first cell. Downstream of the last cell has sufficient capacity to allow vehicles to move away from the last cell. Between any pair of adjacent cells, the number of vehicles can flow to the next cell subject to the constraint:

$q_i(t) = min\{(n_{(i-1)}(t), Q_i(t), N_i(t) - n_i(t)\}s$ ----------

(2.17)

where,

$n_{(i-1)}(t)$: the number of vehicles in cell (i-1) at time t

$Q_i(t)$: the capacity flow into i for time interval t, and

$N_i(t) - n_i(t)$: the amount of empty space in cell i at time t.

Details of the formulation of this model will be discussed in chapter 4.

Variations on the CTM theme can be found in literature. In [38] the asymmetric cell transmission model (A-CTM) is presented. This work also describes a convex optimization problem whose solution is an optimal ramp metering strategy. The linear hybrid system approach called switching mode model (SMM) based on CTM is introduced in [39].

Later Daganzo [40] introduced a new version of the model called lagged CTM (L-CTM) which enable variable cell lengths and adapts a non-concave flow–density.

Szeto [41] modified L-CTM into an enhanced L-CTM which removes few of its drawbacks like negative densities or densities greater than jam density by adding two terms. One is sending function and another is receiving function.

Hui et al. [42] introduced a Variable CTM that includes two parameters, namely, cell length and cell density and obeys the flow conservation law hence reduces the computational burden of the model. This model also includes three different kinds of cell connections with three different expression including simple connection, merge connection and diverge connection. VCTM also includes variable cell length, which allows the use of this model more versatile.

Ziliaskopoulos and Lee [43] adapt CTM for arterial modelling. The cell length is generally much shorter for arterials than for freeways, hence the sampling period Δt must be small enough to ensure;

$$v\Delta t < l \quad \text{---------- (2.18)}$$

Where, v is the free flow speed and l is the cell length.

In the location specific CTM by Chen et al. [44], a modified CTM is used to take into account the model variability influenced by sensor locations, geometry features and many other factors. Using various shapes of fundamental diagrams, the phenomena like capacity drops, lane-by-lane variations, non-homogeneous wave propagation velocities and temporal lags can be reproduced.

Long et al. [45] used the concept of CTM to simulate the formation and dissipation of traffic jams at the microscopic level. In particular, this model focuses on jam propagation and dissipation in two-way rectangular grid networks. In the model, the downstream exit of the link is channelized to represent the interactions of vehicles in different directions. The proposed model includes two components: the cell inflow model and the flow conservation model and used two measures, namely, traffic jam size and congestion delay to explain the effect of congestion. The simulation results show that there are two strategies to minimize jam size and reduce time for jam dissipation:

(1) reduce the length of channelized area and, (2) allocate the stop line widths for all directions in the same ratio as the demands.

Tiriolo et al. [46] developed new traffic flow model CTM-UT (Cell Transmission model for Urban Traffic), based on cell transmission concept, to capture urban traffic dynamics taking into account complex flow interactions among lane groups at upstream of signalized intersections. This model is designed to simulate, at macroscopic level, more realistically the dynamic interaction of queues among neighbouring lanes and intersections for large scale urban network. Model validation has been undertaken by comparing with VISSIM results obtained in different scenarios that have been tested.

To enhance CTM, a conditional cell transmission model (CCTM) is developed by Wang [47] with two improvements. First, CTM is expanded for two-way arterials by taking account of all diverge and merge activities at intersections. Second, a conditional cell is added to simulate periodic spillback and blockages at an intersection. The cell exists conditionally, depending on whether or not there is a spillback at an intersection. In other words, if spillback happens, the conditional cell exists and stores the vehicles which spill back into the intersection; if there is no spillback, the conditional cell will not exist. In CCTM, users may input the probability of a conditional cell (drivers breaking the driving rule) and probability of occurrence of useful location of a gap to match the characteristics of local drivers' behaviour. The CCTM traffic flow simulation was initially developed using evolutions of small model of six cell mode. It included (a segment cell, a diverge cell, a cell in front of an intersection, a cell in a left turn lane, a cell in the minor street and a conditional cell). They were loaded with light duty traffic, moderate duty traffic and heavy-duty traffic respectively. To test the overall performance of CCTM, a series of experiments are designed and performed for a

multilane, two-way, three-signal sample network. Experiments were conducted to give sensitivity analyses to four user-defined parameters including traffic demand, traffic signal timing, possibility of occurrence of a useful gap and possibility of a conditional cell. The results demonstrate that CCTM can accommodate various traffic demands and CCTM's accurate representation of traffic flow.

Huang [48] introduced a new CTM-based model named CTM-URBAN to address the short travel time prediction error in urban roadway and to provide a generic framework for future development of CTM in simulation of urban traffic flows. CTM-URBAN incorporates: a new diverge algorithm that permits modelling of multiple movements and multiple signal phases; a new mechanism to generate dynamic turn ratios instead of present static values; the ability to simulate lane blockage and full blockage at intersections which improves the realism of the simulation under congested traffic conditions; and time-based input parameters allowing more realistic and flexible representation of various traffic condition and operation scenarios. All these features of CTM-URBAN and other minor improvements make the simulator more suitable for real-time simulations compared with the basic version of CTM.

Skabardonis and Geroliminis [49] propose an analytical model for travel time estimation on arterials. Their model is based on CTM, desribes the spatial and temporal queuing at traffic signals and explicitly considers the signal coordination in estimating traffic arrivals at intersections. It estimates the travel time over an arterial link as the sum of free flow time and the delay at traffic signal.

Feldman and Maher [50] investigate CTM applicability to the network of signalized arterials and compare it with the TRANSYT model. Modelling the arterial with a pair of traffic signals with both CTM and TRANSYT, the authors conclude that CTM yields similar orcbetter results than TRANSYT does.

Lo [51] transforms CTM into a set of mixed-integer constraints and casts the dynamic signal-control problem to a mixed-integer linear program. As a dynamic platform, this formulation is flexible in dealing with dynamic timing plans and traffic patterns. It derives dynamic as well as fixed timing plans and addresses pre-existing traffic conditions and time dependent demand patterns.

Amasri and Friedrih [52] also apply CTM to urban arterials and compare it with queuing models. They use genetic algorithm (GA) to and optimal signal timing plan having CTM as an underlying traffic flow model.

Lin & Ahanotu [53] compared the performance of the CTM under both congested and non-congested traffic conditions with data collected from a continuous segment of freeway I-880 in California. It was found that in free-flow condition, CTM provides as high as a 0.9 correlation value at a sampling interval of 6 seconds and asymptotically tends to a perfect correlation at large sampling intervals. Again, a density-based modified version (Muñoz et al.,[54]) of the CTM produced density estimates which showed only 13% mean error (averaged over all the test days) with measured densities on I-210 West in Southern California during the morning rush-hour period.

Stochastic Cell Transmission Model (SCTM) proposed by Sumalee et.al. [55], is used to model traffic flow density on freeway segments with stochastic demand and supply. The SCTM consists of five operational modes corresponding to different congestion levels of the freeway segment. Each mode is formulated as a discrete time bilinear stochastic system. A set of probabilistic conditions is proposed to characterize the probability of occurrence of each mode. The overall effect of the five modes is estimated by the joint traffic density which is derived from the theory of finite mixture distribution. The SCTM captures not only the mean and standard deviation (SD) of

density of the traffic flow, but also the propagation of SD over time and space. An approximately two-miles freeway segment of Interstate 210 West (I-210W) in Los Ageles, Southern California, is chosen for the empirical study. Traffic data is obtained from the Performance Measurement System (PeMS). The stochastic parameters of the SCTM are calibrated against the flow–density empirical data of I-210W. Both the numerical simulation results and the empirical results confirm that the SCTM is capable of accurately estimating the means and SDs of the freeway densities

Alecsandru in [56] suggests some modification to CTM that include microscopic features such as disaggregating the traffic flow by lanes and explicitly modelling the effects of individual lane-changing manoeuvres; replacing some of the original parameters in the analysed network with stochastic variables to capture the effect of the random driving behaviour; and changes to the model equations that allow to keep track of different vehicle types. He also compares this modified CTM with CORSIM microsimulation, and shows that the simulation outputs of these two models match well.

Kimms, A. and K.-C. Maassen [57] formulate an optimization problem for evacuation that is more general than previous work for computing possible traffic routes in complex street networks as well as assignments to safe destinations, and solve it from Daganzo's idea of CTM by considering road sections and flows between these sections. The cell transmission model is modified for optimization problem like this. Later [58] the extended Cell-Transmission-Based Evacuation Planning Model (Ex-CTMPM) a new optimization model is developed to facilitate the previous in terms of choosing the optimum cell size. This modelling approach takes advantage of a standalone vehicle reallocation optimization model and additional traffic flow limitations.

CTM can also be used in dynamic traffic assignment (DTA). Most of the existing analytical DTA formulations mostly use macroscopic link travel time functions to model traffic. However, it is difficult for such functions to capture traffic interactions across multiple links such as queue spillbacks and dynamic traffic phenomena such as shock waves. In this situation, Lo H.K. [59] formulate a new model after the CTM, which provides a convergent approximation to the LWR [4] model and covers the full range of the fundamental diagram. This study transforms CTM in its entirety to a set of mixed-integer constraints. The significance of this is that it opens up CTM to a wide range of dynamic traffic optimization problems, such as the Dynamic User Optimal (DUO) formulation and dynamic signal control.

Hadiuzzaman et. al. [60] developed DynaTAM—a field application tool which can be used to analyze, simulate, and optimize traffic network in off-line or on-line mode for Active Traffic Demand Management (ATDM). This tool provides Variable Speed Limit (VSL) and Ramp Metering (RM) control as the start-up ATDM strategies with a hierarchical and coordinated control system. It evaluates the traffic states for roadway links by the METANET and CTM. These macroscopic traffic models work as reference traffic simulators for traffic state prediction.

Another important application of CTM is in traffic capacity. VSL can be used on freeways to manage traffic flow with the goal of improving capacity. An analytical model based on the CTM is developed by Hadiuzzaman and Qiu [61] to understand the effectiveness of the VSL control. Two modifications in the FD are proposed in the model: (1) active bottleneck in which there is a capacity drop once feeding flow exceeds its capacity; and (2) variable free-flow speeds for the cells operated with VSL control. Lcaza A. et.al. [62] developed Hysteretic Cell Transmission Model (HCTM) based on CTM and incorporates a feature to reproduce the capacity drop phenomenon

observed in real traffic. An auxiliary dynamic state is included that induces hysteretic behaviour on the density-flow relationship. The hysteresis is dependent on the time derivative of the density in a particular cell and allows to change the congested flow traffic wave velocity in the fundamental diagram and, with this, to produce a capacity drop.

First-order traffic models can capture most of the important traffic flow characteristics, such as formation and dissipation of shock waves. However, as noted by Zhang[63], Gartner et al.[33] and other related studies, the first-order models are unable to capture traffic instability, driver's delayed response to traffic conditions and their anticipation behaviour. To overcome these shortcomings and to improve the accuracy level provided by first-order models, second-order models were developed.

2.4.2 Second-Order Macroscopic Traffic Models

While the first-order macroscopic traffic models are characterized by a single dynamical partial differential equation for flow and density, and the speeds are derived from a static speed-density relationship, the second-order models have an independent speed dynamics in addition to density dynamics. Such a speed dynamics describes the local acceleration as a function of speed and/or density as well as other possible exogenous factors.

As early as the mid-1950s, Lighthill and Whitham [4], in their seminal work on kinematic waves, suggested that higher order terms be added to account for some traffic properties, such as inertia and anticipation, and they proposed a general form of a motion equation:

$$\frac{\partial q}{\partial t} + c\frac{\partial q}{\partial x} + T\frac{\partial^2 q}{\partial t^2} - D\frac{\partial^2 q}{\partial x^2} = 0 \quad \text{---------- (2.19)}$$

Where, c is the traffic wave speed, T is the inertia time constant for adjustment of speed, D is the coefficient of diffusion. The authors did not provide an independent speed dynamics for this model.

The most popular second-order model was suggested by Payne [64], which has both speed and density dynamics. He showed that the average speed in a section of a roadway is influenced by three major mechanisms: relaxation, convection and anticipation. Payne approximated individual driver behaviour with the help of the following equation:

$$v[(t+\tau), x(x,t+\tau)] = V_e\{\rho[t, x(t)+\Delta x]\} \quad \text{---------- (2.20)}$$

This equation expresses that the speed of an individual vehicle after a reaction time τ is equal to the equilibrium speed corresponding to the density some distance Δx downstream. After repeatedly applying linear Taylor approximations to Equation 2.20 and using the density at the midway of two vehicles to represent the space headway, the following dynamic equation for the average speed was obtained:

$$\frac{\partial v(x,t)}{\partial t} + \underbrace{v(x,t)\frac{\partial v(x,t)}{\partial x}}_{\text{convection}} = \underbrace{\frac{V_e\left[\rho(x,t)\right] - v(x,t)}{\tau}}_{\text{relaxation}} - \underbrace{\frac{c_0^2(x,t)}{\rho(x,t)}\cdot\frac{\partial \rho(x,t)}{\partial x}}_{\text{anticipation}} \quad \text{---------- (2.21)}$$

$$c_0^2(x,t) = -\frac{1}{\tau}\frac{dV_e\left[\rho(x,t)\right]}{d\rho} \quad \text{---------- (2.22)}$$

Where c_o is the anticipation factor. Payne defined the three different terms of Equation 2.21 as:

- **Convection**: It accounts for the change in average speed at a location due to vehicles leaving or arriving with different speeds.
- **Relaxation**: It describes the tendency of traffic flow to relax to an equilibrium speed, which corresponds to the homogeneous steady state in the flow. It is assumed that an

equilibrium speed $V_e(\rho)$ exists, but the traffic state can deviate from it. When other influences (reflected by the convection and anticipation terms) are small, traffic tends to relax to the equilibrium speed.

- **Anticipation**: It describes driver‘s anticipation on spatially changing traffic conditions (reflected by the spatial variation of density) downstream.

Discretisation and modifications of the Payne model have led to the origin of a family of second-order models like the models of Payne[65], Papageorgiou [66], Lyrintzis et al. [67] and Liu et al. (1998). Among these, the most widely used is the METANET model, which was validated against real traffic data with remarkable accuracy at several instances. For example, Papageorgiou et al. [66] successfully estimated the traffic states of a 6-km stretch of the southern part of Boulevard Périphérique in Paris with standard deviations of only 10.8 km/h for mean speeds and 714 veh/h for traffic volumes. Nevertheless, it was noted that the same parameter values of the exponential FD were used for all links in spite of the different shapes appearing from the field data at different sites.

These second order models account for the driver’s delayed response (relaxation) and convection. The difference lies in the functional form of anticipation or traffic pressure and the viscous term. The models can be generalized as:

Vehicle Acceleration = Relaxation +Convection +Anticipation (or Pressure)+Diffusion (or Viscous term)

2.5 Traffic Flow Models for Heterogeneous Traffic

From the above discussions it becomes evident that the macroscopic traffic flow models are mostly empirical and they have their own pros and cons. Their performances may be very different for different operating conditions; viz. lane-based homogeneous,

non-lane-based heterogeneous etc. Hence, Papageorgiou [68] suggests that the sufficiency of the traffic flow theories be decided depending on the specific utilizations. Within the vast literature on macroscopic traffic flow modelling, surprisingly few studies have addressed the heterogeneous traffic condition prevalent in many developing countries like Bangladesh, India etc. Majority of these researches (e.g. Venkatesan et al. [69], Arasan & Koshy [70], Jin et al. [71], Gunay [72]) mainly focus on the microscopic approach of traffic flow modelling. Other works like (Chari & Badarinath [73] and Gupta & Khanna [74]) focus on developing speed, flow and density relationships for mixed traffic conditions and introduce the concept of 'areal density' instead of linear density measurements.

A very limited number of first-order macroscopic models have also been developed for heterogeneous traffic. For instance, (Nair et al. [75]) views the disordered, heterogeneous traffic system as granular flow through a porous medium and extends the LWR theory using a new equilibrium speed-density relationship. This relationship explicitly considers the pore size distribution, enabling the model to successfully capture the 'creeping' phenomena of heterogeneous queues. However, a microscopic simulation of vehicle configuration is used to determine the pore space distribution and detailed trajectory information of the disordered traffic stream is required for model calibration.

Tuerprasert et.al. [76] propose a new mathematical model of macroscopic road network mobility, based on CTM. He contend that the standard CTM (S-CTM) cannot capture the mixed composition of vehicle types (e.g. truck, car, bus or smaller vehicles), which is a vital concept for practical applications. He named CTM that includes vehicle type as Multiclass CTM (M-CTM) and incorporated vehicle class-wise speed variations. Further report on a study in which both S-CTM and M-CTM are compared

with the simulated result at the microscopic level from MITSIM software [77]. The results suggest that M-CTM is more accurate than S-CTM, particularly in uncongested networks with non-stationary vehicle composition without compromising on the computational complexity.

Ngoduy [78] noticed that most of the existing first order continual model cannot display the classwise (i.e. car, bus etc.) widely scattered flow-density relationsionship. He considered this relationship due to random varuations in driving behaviour. But this randomization can be modelled by stochastic setting of random parameters i.e. capacity hence he proposed stocustic fundamental diagram. The numerical simulation with global parameters has revealed that the proposed model is able to capture the real traffic dynamics but it gives the computational complicacy.

Liu et. al. [79] provides an analytical formulation for a mixed traffic system that includes cars and buses, which realistically replicates moving bottlenecks (MB) as well as route choise. They modify the original lagged CTM [40] to BUS-CTM and make it to recognize speed differentials between the free-flow speed of buses and cars. A set of speed ratios were considered between the vehicle classes, where the free-flow speed of the fastest vehicle class was no more than two times that of the slowest vehicle class. In addition, they add capacity reduction phenomenon in CTM caused by buses hence replicate the moving bottlenecks caused by buses within the CTM framework. Using these assumptions, the model divided the original cells into sub-cells to account for the speed differentials of the vehicle classes during simulation. The numerical simulation of the model suggests that the BUS-CTM obtains more realistic results compared with the application of the traditional CTM in a mixed car–bus transportation system.

Another extension (Wong & Wong [80]) of the LWR model takes into account the dynamic behaviour of heterogeneous users according to their choice of speeds in a

traffic stream. The model uses an exponential form of speed-density relation and can replicate many puzzling traffic flow phenomena such as the two-capacity (or reverse-lambda) regimes occurred in the fundamental diagram, hysteresis and platoon dispersion. However, being extended versions of the first-order LWR model, neither of these models have independent speed dynamics and they lack field validation.

2.6 Chapter Summary

This chapter provides an overview of state-of-the-art of traffic flow models with a special focus on first-order macroscopic flow models and its implication in different traffic conditions. The traffic models are reviewed with respect to their categories in terms of *level of detail*, *scale of independent variables*, *nature of independent variables* and *model representations*. Most of these models are developed for lane-based car dominated operating condition. A limited number of first-order macroscopic models for heterogeneous traffic are found from the extensive literature review but those are continuum in nature. Hence, this research work aims at introducing a first-order flow discrete model for heterogeneous traffic which is expected to show better accuracy in estimation of the complex traffic dynamics of Dhaka city.

CHAPTER 3

DATA COLLECTION AND PROCESSING

This chapter presents details of the selected study site and the high-resolution data collection as well as processing techniques adopted for the research. Later the collected data will be used for calibration and validation of the macroscopic model in the later part of this research. Some justifications regarding the choice of methods employed are also provided in this chapter.

3.1 Study Area

The study site is the Tongi Diversion Road, a section of the Dhaka-Mymensingh Highway (N3) in Bangladesh (shown in Figure 1.1). It is an 8-lane major artery road in Dhaka, which connects the capital city with the Shahjalal International Airport. The selected 3.26 kilometres (km) long uninterrupted section has one off-ramp, closely followed by an on-ramp. These form one diverge and one merge sections along the corridor. There are exactly 4 through lanes on each direction of the test site totalling up to a width of 14.48 metres (m) to 14.94 m in different links. The on and off ramps have two lanes each, though lane discipline is absent in the main stream flow and in the ramp flows. The test section experiences a directional average annual daily traffic (AADT) of about 11451 vehicles. The traffic stream consists of 40% cars, 12% microbuses or jeeps, 10% motorcycles, 8% buses, 10% utility vehicles and 20% auto-rickshaws. Such geometric and traffic characteristics make the test site an ideal study location for non-lane-based heterogeneous uninterrupted traffic condition.

3.2 Data Collection

Collection of high-resolution traffic data under the existing traffic condition of the study area is a very challenging task. Because the existing traffic is non-lane based and

heterogeneous in nature. This difficulty arises because the loop detectors are unsuitable for the test site due to measurement errors caused by non-lane-based movement of vehicles e.g. vehicle will activate either both or neither of two adjacent detectors. Moreover, traffic cameras for vehicle detection are absent along the corridor. Under these circumstances, video cameras are installed at various locations of the study site to provide traffic data for the research through image processing technique.

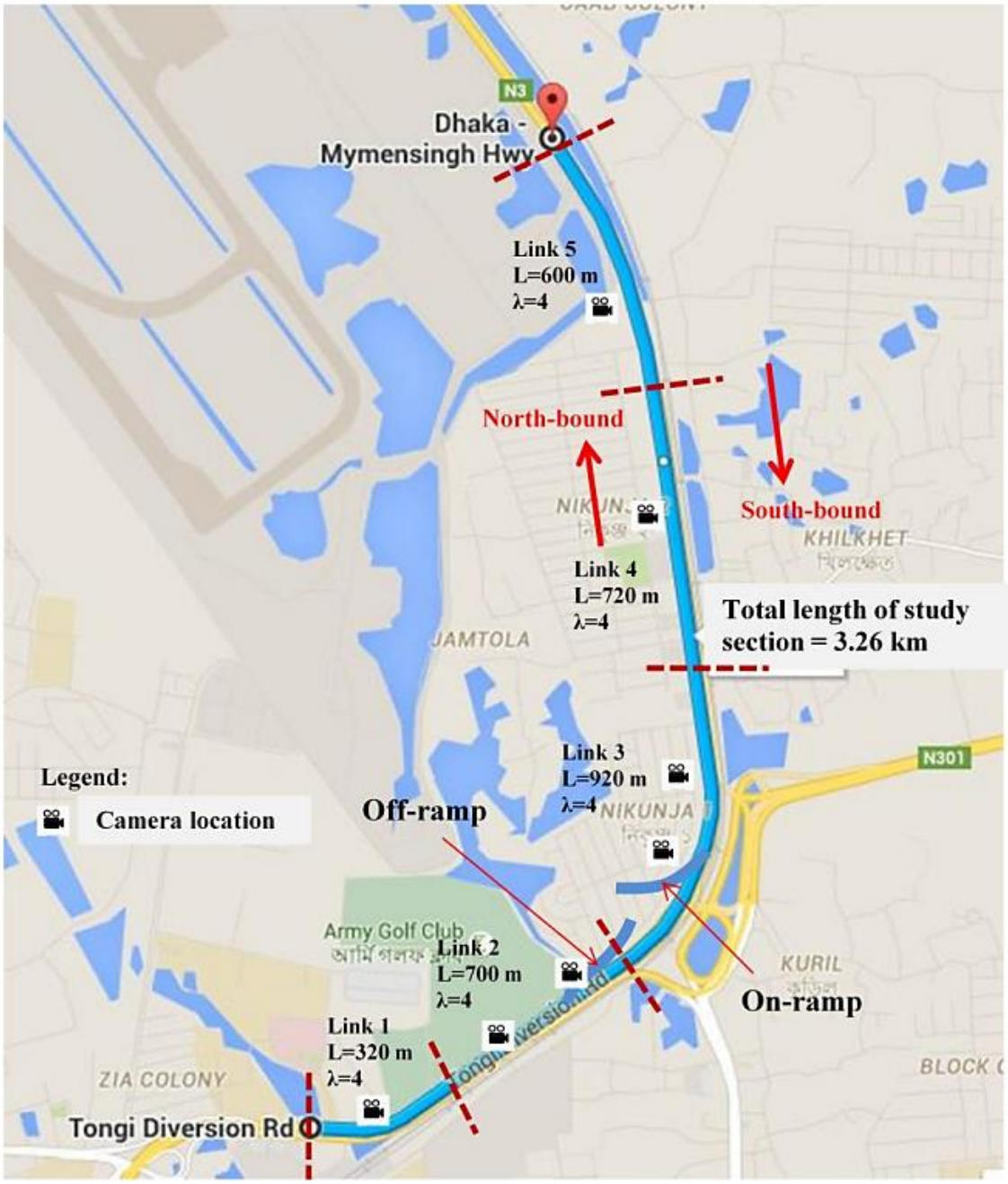

Figure 3.1 Discretization details of the study area.

For macroscopic simulation, the corridor is discretized into five links with the lengths varying from 320 m to 920 m as shown in Figure 3.1. The off-ramp is located at the end of link 2 and the on-ramp is located at the beginning of link 3. Five video cameras are installed along the mainline, one at approximately mid-length of each link. The data obtained from each camera is considered representative of the traffic condition of the whole link. The ramps are also equipped with video cameras for collecting data of the merging and diverging traffic. The approximate locations of the cameras are also indicated in Figure 3.1 whereas the details of each camera location can be found in Figure 3.2 (a-h).

Although the non-lane-based heterogeneous behaviour becomes more acute with the increase of traffic volume in the roadway, the test site was videoed from 3:00 PM to 6:00 PM covering both peak and off-peak periods for FD investigation. Two sets of videos were collected for the same time period on 15th and 16th April, 2015. These videos were processed and the extracted data was filtered for anomalies. Ultimately, 2.5 hours data of 15th April was used for calibration of the model parameters and the similar data set from 16th April was used for model validation. To ensure better quality of the collected data, the camera height and angle of projection were strictly maintained.

Figure 3.2 (a) Camera location on Link 1

Figure 3.2 (b) Camera location on Link 2

Figure 3.2 (c) Camera location on Link 3

Figure 3.2 (d) Camera location on Link 3 (close-up)

Figure 3.2 (e) Camera location on Link 4

Figure 3.2 (f) Camera location on Link 5

Figure 3.2 (g) Camera on off-ramp (above); Field of vision of the camera (below)

Figure 3.2 (h) Camera location on on-ramp showing details of the data collection process

As shown in Figure 3.2 (h), the mounting heights of the cameras were at least 20ft to reduce the object details detected by the image processing algorithm and the camera angle was less than 45 degrees to avoid perception problem. However, the angle was not so small as to cause restriction in vision. Due to the absence of suitable vantage points meeting such requirements in links 1, 2, 4 and the on-ramp location, cranes were used for mounting the cameras at the required height for a period of 3 consecutive hours each day. The presence of foot over bridges of sufficient height in links 3 and 5 and on the off-ramp location allowed the data collection process to be carried out without the use of cranes.

3.3 Data Processing

For extracting, high-resolution traffic data from the video footages, an object detection algorithm has been used which operates based on the Background Subtraction (BGS) technique of image processing[81]. The developed algorithm can successfully detect non-lane-based movement of vehicles. It can also identify non-motorized traffic, dark car and shadow quite accurately. Video data and vehicle geometry are provided as input to the algorithm and it gives vehicle count and time mean speed at required intervals as the output. For measuring flow, strip based counting method combining successive incremental differentiation is used. On the other hand, for measuring speed, the algorithm segments the whole field of vision and detects the change in centre of area of an object in each segment to find the corresponding pixel speed. Then calibrating the pixel distance with the field distance, instantaneous and time mean speeds are obtained, which can easily be converted to space mean speed. The density of the traffic stream for the research is estimated from the measured flow and speed.

The developed algorithm has been proved to give highly accurate traffic data with Mean Absolute Error (MAE) of only 14.01 and 0.88 in flow and speed measurements respectively when compared with actual field measurements. The algorithm addresses some of the major problems faced in the BGS technique, like the camouflage effect, camera jitter, sudden illumination variation, low camera angle and elevation etc. The process of traffic detection by the algorithm is briefly illustrated below.

3.4 Traffic Detection Technique

The background modelling algorithm used for traffic detection in this research is quite simple, yet accurate. It involves the use of static frames for object extraction from a video stream or image. Traffic is detected according to the following basic steps.

Step 1: Choosing the static background model (B)

This is the primary step of static background subtraction technique. The background model is a frame within the video having no traffic in it. This background is selected up careful inspection of the video. Figure 3.3 (a) shows such a background model used for traffic detection from the video of the off-ramp location of the study site.

Figure 3.3 (a) The background model (B).

Step 2: Selecting the frame (I) on which vehicle detection is to be performed

Using an iteration process, the frame on which the detection should be performed is to be selected one by one from the video file. Figure 3.3 (b) shows a typical frame for traffic detection.

Figure 3.3 (b) A random frame (I) for vehicle detection.

Step 3: Determining the absolute difference (D) between B and I

The difference between the static background model B and the traffic detection frame I gives the differential image where only the traffic exists. For example, Figure 3.3 (c) is the differential image of the frame I of Figure 3.3 (b).

Figure 3.3 (c) The differential image (D) of frame I

Step 4: Converting differential image into binary image

In order to make the differential image machine readable, it is converted into binary image using a "threshold value". The selection of proper threshold value is very important for accurate vehicle detection. In the differential image, the pixels having intensities lower than the selected threshold is assigned value "0", whereas those having intensities higher than the threshold are assigned "1". Thus the differential image gets converted into a binary code as in Figure 3.3 (d).

Figure 3.3 (d) The binary image of D

Step 5: Performing morphological operation

Next, some morphological operations are required for enhancing the quality of the binary image by removing unwanted "noises". For this purpose, binary opening is used. Its magnitude depends on the type of opening algorithms used i.e. square, circular, disk type opening etc. On the other hand, binary closing is needed to recover an object from the binary image. Its magnitude depends on the same factors as opening. The improvement of the quality of binary image after applying opening and closing are shown in Figures 3.3 (e) and (f) respectively.

Figure 3.3 (e) Binary image after applying opening

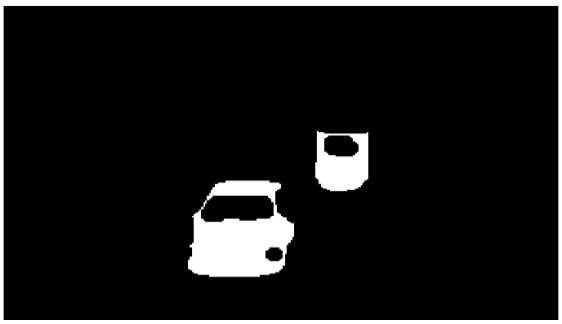

Figure 3.3 (f) Binary image after applying closing

Thus the vehicles from a video stream are extracted according to these steps, analyzing one frame at a time. Then applying the counting and speed measurement techniques mentioned earlier, the flow and speed data in the field condition are obtained at the required time interval (20 seconds for this research).

3.5 Chapter Summary

This research aims at developing a macroscopic flow model for the non-lane-based heterogeneous traffic condition of Dhaka city. For this high-resolution data is the prerequisite. The current chapter introduced the test section used in this research along with details of the video-based data collection method adopted. It then briefly discussed the image processing technique used here for extracting flow and speed data from the video footages of the test site. The measured high-resolution data will be used for the development and analysis of the model in the subsequent chapters.

CHAPTER 4

MODEL DEVELOPMENT AND ANALYSIS

Macroscopic continuous traffic flow models, as discussed earlier in Chapter 2, represent traffic as a compressible fluid in terms of speed, flow and density, as opposed to microscopic models, which on the other hand reproduce the behaviour of individual vehicle as its driver, responds to its environment by changing its speed and lane. The popularity of macroscopic modelling approach is based on easy implementation, fast to run simulation and allowing the user to simulate many different traffic situations in relatively short span of time. The present chapter focus on the development of such macroscopic model for heterogeneous non-lane-based traffic condition of Dhaka city. Our model choice is the first order CTM [3] which will be used as the base model in this research. Then the nature of the traffic flow for heterogeneous operating condition is investigated utilizing the collected field data. Based on the results of this investigation, a modified CTM is proposed, which is then calibrated and validated to accurately simulate the urban traffic system of Dhaka city and expected to simulate traffic of same nature.

4.1 The Basic Cell Transmission Model

First, assume that, CTM will evaluate traffic over a one-way road without any intermediate entrances or exits, so that vehicles enter at one end and leave at the other. This will simulate the system with a “time-scan” strategy where current conditions are updated with every tick of a clock.

Let us assume that, the road is divided into homogeneous sections (cells), numbered consecutively starting with the upstream to end of the road, from i = 1 to I.

The lengths of the sections are not chosen arbitrarily; they are set less than the distances travelled by a light traffic of typical vehicle type in one clock tick.

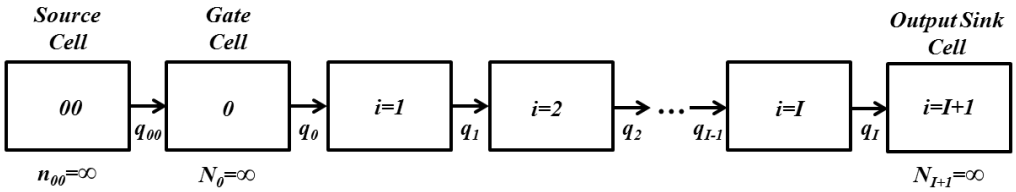

Figure 4.1 Ideal Highway Section for Basic CTM.

Vehicles under light traffic category then in a cell can be assumed to advance to the next with each tick; it is unnecessary to know where within the cell they are located. Thus, the system's evolution obeys the conservation law:

$n_{i+1}(t+1) = n_i(t)$---------- (4.1)

In equation 4.1, $n_i(t)$ is the number of vehicles in cell i at time t. We will assume that the above expression stands for all flows, unless traffic is slowed down by queuing from a downstream bottleneck. This assumption seems reasonable because, for crowded conditions as it might arise during the rush hour, most of the delays occur due to queuing at bottlenecks where flow temporarily exceeds capacity, rather than to any dependency between flow and speed.

To incorporate queuing we introduce two constants: $N_i(t)$, the maximum number of vehicles that can be present in cell i at time t, and $Q_i(t)$, the maximum number of vehicles that can flow into cell i when the clock advances from t to $(t + 1)$. The first constant is the product of the cell's length (l) and its "jam density" (ρ_{jam}) and the second one is the minimum of the "capacity flows" or "critical flow" (q_c) of cells $(i - 1)$ and i. It will be called the "capacity" of cell i which represents the maximum flow that can be transferred from $(i - 1)$ to i. We allow these constants to vary with time to be able to model different traffic incidents. The number of vehicles that can flow from cell $(i - 1)$ to cell i when the clock advances from t to $(t + 1)$, flow $q(t)$, is assumed to be the smallest of three quantities:

$n_{(i-1)}(t)$: the number of vehicles in cell (*i-1*) at time *t*

$Q_i(t)$: the capacity flow into *i* for time interval *t*, and

$N_i(t) - n_i(t)$: the amount of empty space in cell *i* at time *t*.

Now CTM considers a recursion where the cell occupancy at time (*t+1*) equals its occupancy at time *t*, plus the inflow and minus the outflow; i.e.

$n_i(t + 1) = n_i(t) + q_i(t) - q_{i+1}(t)$ ---------- (4.2)

Where the flows are related to the current conditions; at time *t* as indicated below:

$q_i(t) = min\{(n_{(i-1)}(t), Q_i(t), N_i(t) - n_i(t)\}$ ---------- (4.3)

The simulation would step through time, updating the cell occupancies with each tick of the clock.

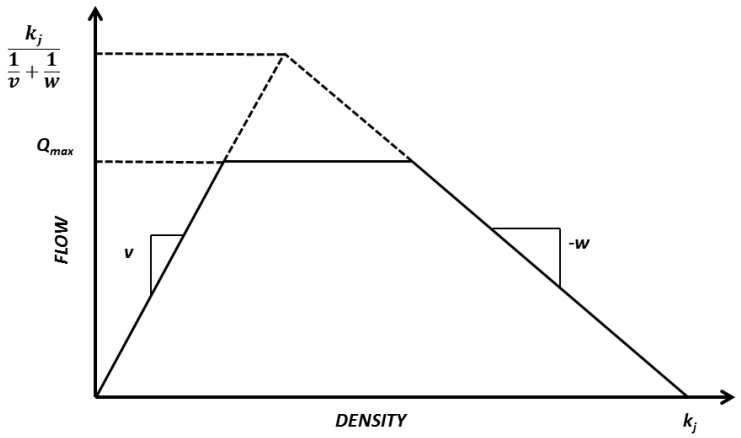

Figure 4.2 The basic Fundamental Diagram.

Boundary conditions can be specified by means of input and output cells. The output cell, a sink for all exiting traffic, should have infinite size ($N_{(I+1)} = \infty$) and have a suitable, possibly time-varying, capacity. Input flows can be modelled by a pair of cells. A "*source*" cell, numbered as"*00*", with an infinite number of vehicles ($n_{00}(O) = \infty$) that discharges into an empty "*gate*" cell "*0*" of infinite size, $N_0(t) = \infty$. The inflow capacity $Q_o(t)$ of the gate cell is set equal to the desired link input flow for time interval *(t + 1)*. The gate cell then acts as a metering device that releases traffic at the desired rate while holding any flow that is unable to enter the link.

Here, the result of the simulation is independent of the order in which the cells are considered at each step. This important property of the CTM will permit the analysis of complex networks, e.g., with loops. The property arises because we are specifying that the number of vehicles that enter a cell is unrelated to the number of vehicles that will leave it; thus, only current conditions influence the inflow to a cell. The vehicles discharges through the sink from the last cell and the empty slots or queue for cars travel backwards at a finite speed, the wave propagation speed, which is not greater than the free flow speed. Therefore, the effects of the outflow should only be noticed upstream after some time. Because this lag is one tick of the clock for our model, this also assumes that density waves propagate backwards at the free flow speed.

Now, we consider networks where the maximum number of *links* entering and/or leaving a cell is 3. Thus, cells can be classified into three types: "diverge" if only one link enters the cell but two leave it, "merge" if two links enter and one leaves, and "ordinary" if one enters and one leaves.

The basic modelling block, a three-legged junction, will consist of the merge/ diverge cell, the two links entering/ leaving it and the two cells at the other end of these links. In order to identify all the components of the junction relative to one of its links (k), the prefixes "c" and "C" will be used: "ck" will denote the other link in the modelling block, and "Ck" the third cell.

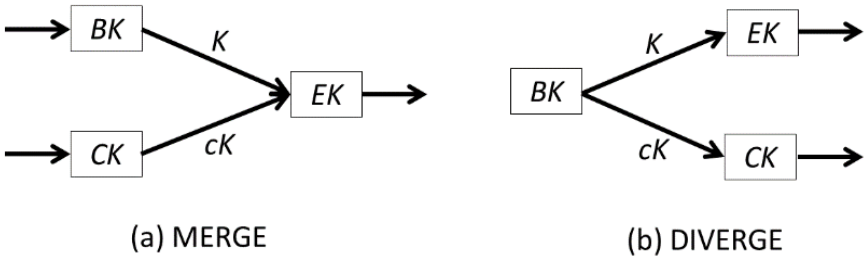

Figure 4.3 Representation of Merge and Diverge.

4.1.1 Ordinary links

If we let, $q_k(t)$ denote the flow on link k from clock tick t to clock tick $(t+1)$, and δ_I the wave speed coefficient of cell I , then:

$q_k(t) = min\{ n_{Bk} , min[Q_{Bk},Q_{Ek}] , \delta_{Ek}[N_{Ek}-n_{Ek}]\}$ ---------- (4.4)

We can define, for simplicity that,

$S_I(t) = min\{Q_I, n_I\}$---------- (4.5)

$R_I(t) = min\{Q_I, \delta_I[N_I-n_I]\}$ ---------- (4.6)

Where, Q_{Bk}, Q_{Ek} are capacity of cell BK and EK, $S_I(t)$ and $R_I(t)$ are density at time t of sending cell and receiving cell respectively.

4.1.2 Merges

In the real world, a merge can be in one of three possible waves:
(a) **Forward**: If the flow on both approaches is dictated by conditions upstream then the waves move forward.

(b) **Backward**: If the flow on both approaches are dictated by conditions downstream then waves move backward.

(c) **Mixed**: If the flow is dictated by conditions upstream for one approach and downstream for the other.

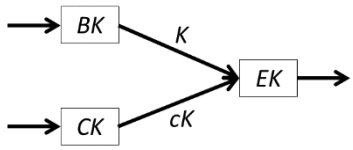

(a) MERGE

Figure 4.4 Merging Cells.

Case (a) arises if both approaches are flowing freely. Case (b) arises when both approaches are congested due to the junction's lack of capacity, or to congestion

downstream. Case (c), which is less common, arises when an approach with priority crowds out traffic on its complementary approach. Given the maximum flow that can be emitted by the two sending cells (S_{Bk} and S_{Ck}), the boundary equations should specify the advancing flows q_k and q_{ck} as a function of the maximum flow that can be received immediately downstream: R_{Ek}. (The variables S_{Bk}, S_{Ck} and R_{Ek}, which capture the current state of the system at the junction, are representing the traffic densities at the junction). Therefor the flow must satisfy the following conditions:

$q_k(t) \leq S_{Bk}$ ---------- (4.7)

$q_{ck}(t) \leq S_{Ck}$ ---------- (4.8)

$q_k(t) + q_{ck}(t) \leq R_{Ek}$ ---------- (4.9)

If the condition in equation 4.9 is not satisfied, we will assume that the maximum possible number of vehicles, R_{Ek}(t), advances into link *Ek*. As long as the supply of vehicles from both approaches, S_k(t) and S_{Ck}(t), is not exhausted we will assume that a fraction (p_k) of the vehicles come from Bk and the remainder fraction (p_{ck}) comes from *Ck*. Where the constants "*p*" are characteristics of the intersection that capture any priorities and satisfy the following condition:

$p_k + p_{ck} = 1$ ---------- (4.10)

If the supply of vehicles on one of the approaches is exhausted before the end of the time interval between clock ticks, then the remaining vehicles to advance will come from its complementary approach.

4.1.3 Divergence

In deriving boundary conditions, it should be considered that the left/right turn percentages will in general depend on the mix of vehicle destinations present in the element of flow currently upstream of the junction.

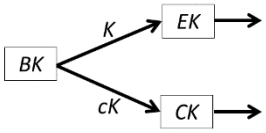

(b) DIVERGE

Figure 4.5 Diverging Cell.

Here we assume that the turning proportions are determined. In figure 4.5, cell *Bk* can send a maximum of $S_{Bk}(t)$ vehicles during time interval $[t,t+1]$ and cells *Ek* and *Ck* can receive a maximum of $R_{Ek}(t)$ and $R_{Ck}(t)$ respectively. These three quantities are still given by equations 4.5 and 4.6. Here, we assume that, the proportions of $S_{Bk}(t)$ going each way are $\beta_{Ek}(t)$ and $\beta_{Ck}(t)$, where, β is the split ratio and $\beta_{Ek}(t) + \beta_{Ck}(t) = 1$.We assume that, split ratio is determined, and traffic flows continuously in this proportion between each clock ticks. Then, flows emitted by the links are:

$$q_k(t) = \beta_{Ek}\, q_{Bk} \quad \text{---------- (4.11)}$$

$$q_{ck}(t) = \beta_{Ck}\, q_{Bk} \quad \text{---------- (4.12)}$$

But these quantities must satisfy the following condition:

$$Flow = max\{\, q_{Bk}(t) : q_{Bk}(t) \le S_{Bk} \,,\, \beta_{Ek}\, q_{Bk}(t) \le R_{Ek} \,,\, \beta_{Ck}\, q_{Bk}(t) \le R_{Ck} \,\} \quad \text{---------- (4.13)}$$

Thus the following condition defines the flow of the diverging cell.

$$q_{Bk}(t) = min\{\, S_{Bk} \,,\, R_{Ek}/\beta_{Ek} \,,\, R_{Ck}/\beta_{Ck} \,\} \quad \text{---------- (4.14)}$$

4.2 Modelling and Calibration of Fundamental Diagram for Heterogeneous Traffic

The fundamental diagram (describing flow-density, speed-density or speed-flow relationship at a given location or section of the roadway) is a basic tool in understanding the behaviour of traffic stream characteristics in macroscopic flow models. In the first order models, speed is derived directly from a steady-state speed-density (v-ρ) FD. Therefore, identifying the nature of this fundamental relationship is a

prerequisite for the development of any macroscopic model. The current section aims at investigating the impact of the non-lane-based heterogeneous traffic condition on FD. More specifically, it will highlight on how the existing traffic flow characteristics of the test site influence the structure and parameters of the FD for the internal links L2, L3 and L4, which will be utilized for modelling purpose.

Over the years different structures of the FD have been proposed depending on the flow conditions and roadway environments. However, it is generally agreed that flow *q* is a concave function of density ρ defined in [*0, p_j*] (*p_j - jam density*); and the corresponding v - ρ relationship is monotone decreasing. Since the FD will be used in the traffic state estimation of the proposed CTM, only the *v-ρ* relationship is investigated in detail in this section. A few functional representations of this relation from the literature are given below.

Greenshields [6] postulated a linear relationship between speed and traffic density based on the data obtained from a rural two-lane Ohio highway. The Greenberg model [5], which is obtained by the integration of car-following model, proposed a logarithmic structure (Equation 4.15), observing speed-density data sets for tunnels. The Underwood model [82] proposed an exponential v - ρ relationship (Equation 4.16) based on the results of traffic studies on the Merritt Parkway in Connecticut.

Greenberg model: $$v = V_m \ln\left(\frac{\rho}{\rho_j}\right)$$ ---------- (4.15)

Underwood model: $$v = V_f e^{-\frac{\rho}{\rho_j}}$$ ---------- (4.15)

Here, ρ_c, V_f and V_m represent critical density, free-flow speed and the speed corresponding to the maximum flow or p_c respectively. Edie [83] suggested that a multi-regime model can be used to represent the traffic breakdown near critical density

ρ_c. He proposed the use of the Underwood model for the free-flow regime and the Greenberg model for the congested-flow regime, thereby overcoming the drawbacks of both of the models. Further developments in the field of FD were directed towards generalizing the modelling approach. Examples of such developments include the one-parameter polynomial model cited by Zhang [63]:

$$v = v_f \left(1 - \left(\frac{\rho}{\rho_j} \right)^n \right) \text{ ---------- (4.17)}$$

And the exponential model used in Papageorgiou et al. [66], which is obtained by adding parameters for data fitting flexibility to the Underwood model.

$$V(\rho) = v_f \exp\left(-\frac{1}{\alpha} \left(\frac{\rho}{\rho_c} \right)^\alpha \right) \text{ ---------- (4.18)}$$

To observe the nature of the fundamental relationship for heterogeneous traffic, the *v-ρ* plots of the field data for different links are fitted with four general structures evident from the literature: namely, the linear, logarithmic, exponential and polynomial forms. Table 4.1 provides a comparative study among these structures, on the basis of their goodness-of-fit. The R-Squared and Root Mean Square Error (RMSE) values reveal that the 3 degree polynomial relationship shows the best fit with the field data for all three links. In relation to the findings of Chari & Badarinath [73], which deduced a logarithmic *v-ρ* relationship with R-Square value of 0.41 utilizing time-lapse photographic data of Hyderabad, India, it can be said that the polynomial structure shows better fit for the prevailing traffic condition.

An in-depth investigation of the above plots reveals that the values of the FD parameters, i.e., v_f and ρ_j vary significantly for different links. In general, the links with greater roadside friction from pedestrian activities on raised sidewalk (as observed for L3 and L4) show lower free-flow speed and greater jam density compared to the link

L2 with less roadside friction. This is because the presence of roadside friction causes sluggish transition from free flow state to congestion state.

Table 4.1 Comparison of Fitness of Different Structures of the Fundamental Diagram in Heterogeneous Traffic Condition

Link No	Goodness-of-fit Parameters	Structure of the Fundamental Diagram (v vs. ρ)				
		$v = a_1\rho + a_2$	$v = a_1 \ln(a_2\rho)$	$v = a_1 \exp(a_2\rho)$	$v = a_1\rho^2 + a_2\rho + a_3$	$v = a_1\rho^3 + a_2\rho^2 + a_3\rho + a_4$
L2	R-Square	0.5800	0.6451	0.6450	0.6364	0.6460
	RMSE	6.1171	5.6233	5.6243	5.6858	5.6254
L3	R-Square	0.4909	0.5951	0.6014	0.5926	0.6036
	RMSE	3.7059	3.3014	3.2791	3.3116	3.2665
L4	R-Square	0.6352	0.6882	0.6969	0.6971	0.7003
	RMSE	4.3238	3.9975	3.9411	3.9442	3.9276

Note: a_1, a_2, a_3, a_4 represent the estimated coefficients of the structures.

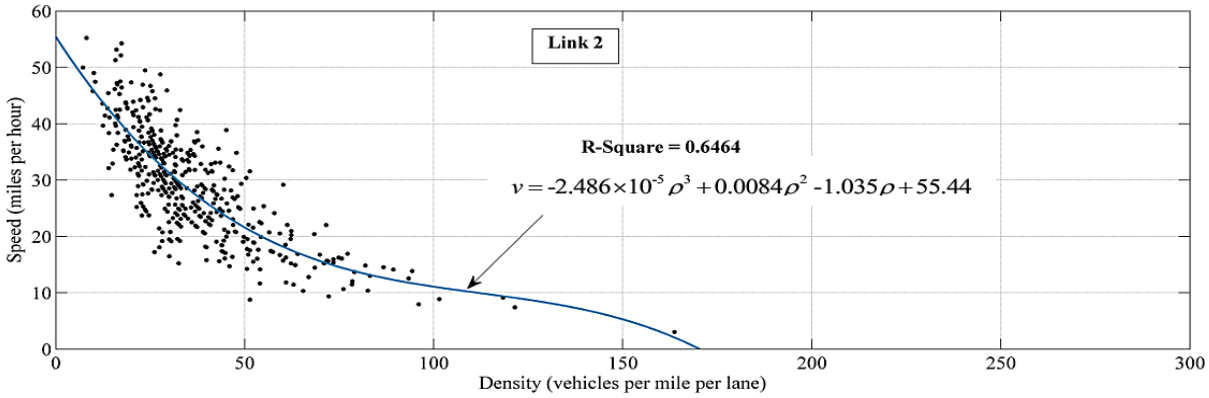

(a)

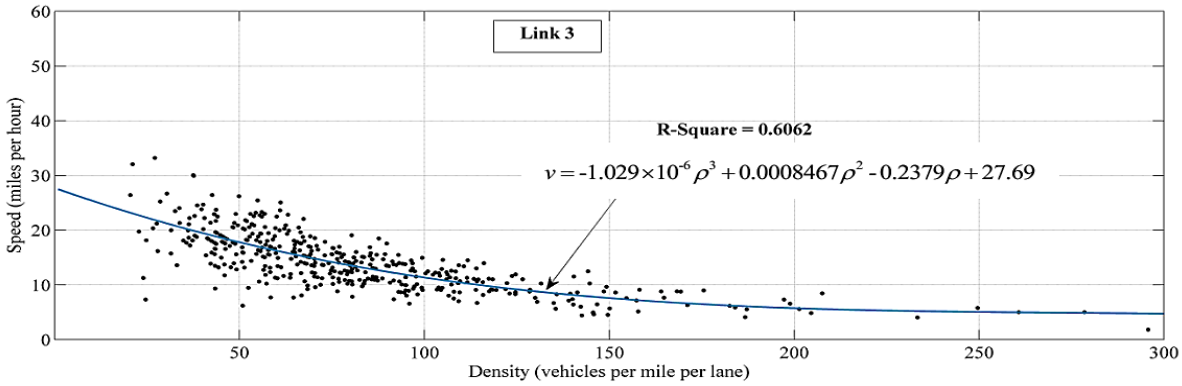

(b)

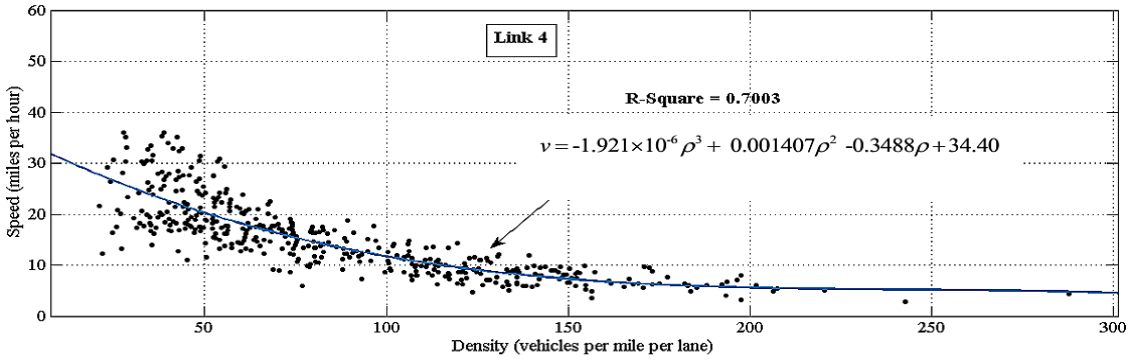

(c)

Figure 4.6 Speed vs. density scatter plots of links 2-4 (20 seconds resolution field data used in the plots was collected from 3:00 PM to 5:30 PM on 15th April, 2015.)

Other forms of FD can be very easily derived from the established relationships. As an example, the flow-density FD of link L2 is derived here. The relationship of link L2 is represented by the following equation:

$$v = -2.486\times10^{-5}\rho^3 + 0.0084\rho^2 - 1.035\rho + 55.44 \quad \text{---------- (4.19)}$$

Multiplying both sides of this equation with ρ yields a functional form of the link's flow q. This is expressed as:

$$q = -2.486\times10^{-5}\rho^4 + 0.0084\rho^3 - 1.035\rho^2 + 55.44\rho \quad \text{---------- (4.20)}$$

Differentiating both sides of equation 4.20 with respect to ρ and then equating it with zero gives:

$$\frac{dq}{d\rho} = -9.944\times10^{-5}\rho^3 + .0252\rho^2 - 2.07\rho + 55.44$$

$$-9.944\times10^{-5}\rho^3 + .0252\rho^2 - 2.07\rho + 55.44 = 0 \quad \text{---------- (4.21)}$$

Solution of equation 4.21 yields the density values for which the flow function's slope is zero. The solutions are ρ = 66, 75 and 112. Hence, the critical density, ρ_c of link L2 is 112 vpml. Putting the value of ρ_c in equation 4.20 gives the capacity of the link. The estimated capacity of the link is 1116 vphl. Similarly, the FD parameters of the other links can also be determined. These are shown in Table 4.2

Table 4.2 Estimated FD Parameters of Different Links

Link	Free flow speed v_f (mph)	Critical density p_c (vpml)	Jam density p_j (vphl)	Capacity f_{max} (vphl)
L2	55.44	112	170	1116
L3	27.69	325	432	1456
L4	34.40	288	376	1371

An interesting observation from the table is that, while the values of ρ_c are quite large, the differences between ρ_c and ρ_j are relatively small. This implies that in heterogeneous operating condition, the critical density is reached rather slowly; but once the density of the roadway reaches this limit, relatively small increase in density causes stagnant congestion of the traffic stream, i.e. the operating speed falls to zero and the jam density is reached. Hence, for the heterogeneous traffic of the test site, the transition from the critical to jam densities is rather abrupt.

4.3 CTMSim: CTM Simulator for MATLab

The first scope of a CTM traffic flow simulator is the ability to compute average speed (v), Flow (q), Density (ρ) very quickly and export the traffic state as accurately as possible. With this aim, a configuration file has been made that contains all physical characteristics of the highway, boundary and initial conditions for simulating CTM. This configuration file allows the simulator to extract highway geometry, estimate data from fundamental diagrams, split ratios for the off-ramps, and generate a demand profile for the on-ramps. For our simulation, the configuration file has been generated using the extracted data described in Chapter 3.

Another goal is to make the simulation interactive, so the user could see the evolution of the freeway state, pause the simulation and change some parameters like fundamental diagram—to simulate an incident and then continue. Interactivity also

helps to calibrate the model, adjust fundamental diagrams, on-ramp demands and off-ramp split ratios where necessary.

4.3.1 The Basic Computational Model

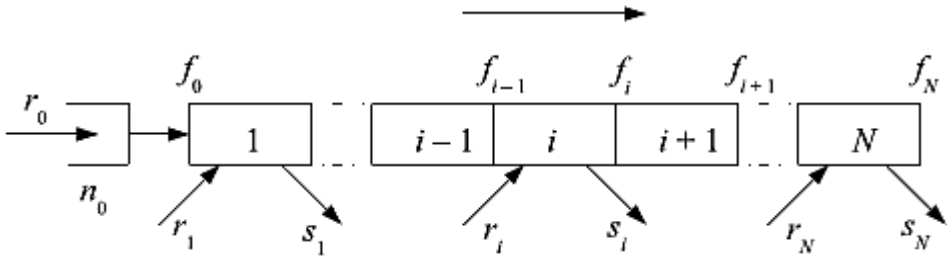

Figure 4.7 The highway configuration with one on- and off-ramp in each cell.

For computation, the model parameters and variables are summarized as below:

Table 4.3: Model parameters and variables used in CTMSIM.

Symbol	Name	Unit
N	Number of cells	dimensionless
Δt	Sampling period (time step)	hours
Δx_i	Cell length	miles
Q_i	Total cell capacity	vehicles per hour (vph)
R_i	On-ramp capacity	vehicles per hour (vph)
S_i	Off-ramp capacity	vehicles per hour (vph)
v_i	Free flow speed	miles per hour (mph)
w_i	Congestion wave speed	miles per hour (mph)
ρ_j	Jam density	vehicles per mile (vpm)
ρ_i^c	Critical density	vehicles per mile (vpm)
β_i	Split ratio	ϵ[0,1], dimensionless
$\overline{\beta}_i$	Complementary split ratio = 1-β_i	ϵ [0,1], dimensionless
γ_i	On-ramp flow blending factor	ϵ [0,1], dimensionless
ξ_i	On-ramp flow allocation factor	ϵ [0,1], dimensionless
k	Period number	dimensionless
$s_i(k)$, $r_i(k)$	Off-ramp, On-ramp flow in cell i in period k	vehicles per hour (vph)
$d_i(k)$	On-ramp demand in cell i in period k	vehicles per hour (vph)
$qu_i(k)$	On-ramp queue size in cell i in period k	no of vehicles
$q_i(k)$	Flow from cell i to i + 1 in period k	vehicles per hour (vph)
$\rho_i(k)$	Density in cell i in period k	vehicles per mile (vpm)
$V_i(k)$	Actual speed in cell i in period k	miles per hour (mph)
$TT(k)$	Travel time in period k	hours

The parameter γ_i, the flow-blending coefficient, determines the influence of the on-ramp flow on the mainline flow that enters i-th cell. It reflects the position of the on-ramp within the cell, with larger values of γ_i corresponding to on-ramps that are closer to the upstream edge. The parameter ξ_i, the flow allocation factor, determines the allotment of available space to vehicles entering from the on-ramp. It reflects the geometrical layout of the cell. For example, if the on-ramp is located at the midpoint, incoming vehicles will only have access to the downstream half of the cell. The on-ramp demand $d_i(k)$ is the number of vehicles per unit of time intending to enter freeway at the *i*-th cell, as opposed to on-ramp flow $r_i(k)$- the number of vehicles per unit of time actually entering freeway at this cell. The initial condition for the simulating the system is the N -dimensional vector of densities $\rho(0)$ at time step 0 . Given the initial condition, on-ramp demands and off-ramp split ratios, CTMSim computes the system evolution in each tick of clock using the following steps:

1. Check if the user-set value of Δt is valid. It must satisfy

$$\Delta t < \min_i \frac{\Delta x_i}{v_i} \quad \text{---------- (4.22)}$$

2. Set time step k = 0.
3. Initialize on-ramp queue size $qu_i(0)$ =0, i = 1...N.
4. Initialize on-ramp flow $r_i(0) = R_i$, i = 1...N.

   In cells without on-ramps, R_i is assumed to be 0.
5. Compute on-ramp flows

$$r_i(k+1) = \min\left\{\begin{array}{l} d_i(k+1) + \dfrac{qu_i(k)}{\Delta t}, \\ \xi_i(\rho_j - \rho_i(k))\dfrac{\Delta x_i}{\Delta t}, \\ R_i, \\ \max\{C(r_i(k)), Q(r_i(k))\} \end{array}\right\}, i = 1...N \quad \text{---------- (4.23)}$$

Where, $C(r_i(k))$ denotes flow value suggested by on-ramp mainline controller

$Q(ri(k))$ denotes the flow value coming from on-ramp queue controller.

6. Update queue sizes.

$$qu_i(k+1) = \max\{qu_i(k) + (d_i(k+1) - r_i(k+1))\Delta t, o\}, i = 1...N \quad (4.24)$$

7. Compute cell-to-cell flows.

$$q_i(k+1) = \min\left\{\begin{array}{l} \overline{\beta_i} v_i(\rho_i(k) + \gamma_i r_i(k+1)\frac{\Delta t}{\Delta x_i}), \\ w_{i+1}(\rho_{j(i+1)}(k) - (\rho_{i+1}(k) + \gamma_{i+1} r_{i+1}(k+1)\frac{\Delta t}{\Delta x_{i+1}})), \\ \frac{\overline{\beta_i}}{\beta_i} S_i, \\ Q_i \end{array}\right\}, i = 1...N \quad \text{---------- (4.25)}$$

8. Compute off-ramp flows

$$s_i(k+1) = \frac{\overline{\beta_i}}{\beta_i} q_i(k+1), if\ \beta_i < 1 \quad \text{---------- (4.26)}$$

$$s_i(k+1) = \min\left\{v_i(\rho_i(k) + \gamma_i r_i(k+1)\frac{\Delta t}{\Delta x_i}, S_i\right\}, if\ \beta_i = 1 \quad \text{---------- (4.27)}$$

9. Compute densities.

$$\rho_i(k+1) = \rho_i(k) + (q_{i-1}(k+1) + r_i(k+1) - q_i(k+1) - s_i(k+1))\frac{\Delta t}{\Delta x_i}, i = 1...N \quad \text{---------- (4.28)}$$

10. Compute actual speeds.

$$V_i(k+1) = \min\left\{v_i, \frac{q_i(k+1) + s_i(k+1)}{\rho_i(k+1)}\right\}, i = 1...N \quad \text{---------- (4.29)}$$

11. Compute travel time.

$$TT(k+1) = \sum_{i=1}^{N} \frac{\Delta x_i}{V_i(k+1)} \quad \text{---------- (4.30)}$$

12. Set k=k+1.

13. Go to step 5.

4.3.2 User Interface

a. Freeway Configuration Editor

To start the freeway configuration editor, the user need to type in MatLab the following

>> fwconfig

If user wish to edit an existing configuration that is stored in the given file, say, myconfig.mat, type;

>> fwconfig myconfig

This brings up a freeway configuration editor window (Figure 4.8), which is partitioned into 12 areas.

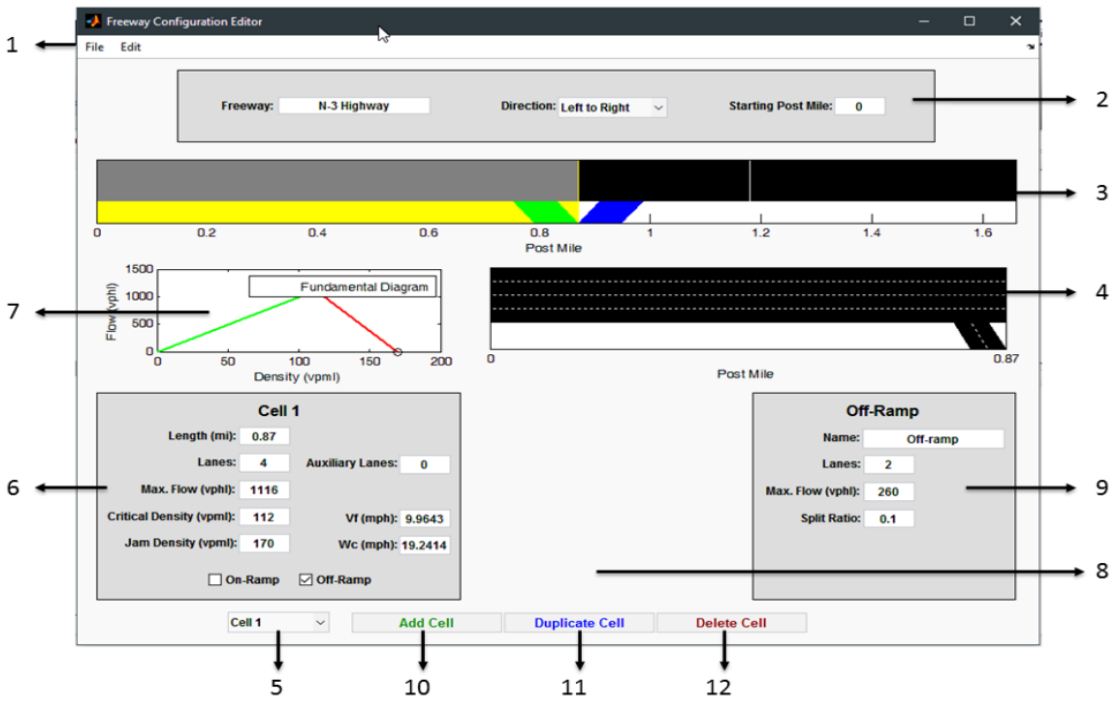

Figure 4.8 Main window of the Freeway Configuration Editor.

1. Menu bar containing the commands listed below.

File

- **New Configuration** – creates new freeway with single cell.
- **Save Configuration** – saves current freeway configuration.
- **Load Configuration** – brings up a file dialog allowing the user to select the CTMSim configuration file for editing.
- **Exit** – closes the program. Prior to this, it brings up a confirmation dialog asking if the user wishes to save current configuration in case it has not been saved already.

Edit

- **Default Cell** – brings up a default cell editor window (Figure 4.9), which allows the user to set up the default parameter values for newly created cells.

Figure 4.9 Default Cell Parameters**.**

2. **General Parameter Panel** – contains parameters defining how the freeway is displayed by the Simulator.

- **Freeway** – a string with freeway name or brief description.
- **Direction** – traffic orientation, left-to-right or right-to-left.

- **Starting Post Mile** – the post mile corresponding to the beginning of the first (most upstream) cell.

3. Freeway layout displays the freeway divided into cells. Each cell is represented by a black rectangle whose horizontal side is proportional to the cell length and vertical side is proportional to the number of lanes in the cell. On-ramps are shown in blue, and off-ramps – in green. The cell that is currently selected is indicated by the yellow background and is colored in gray. To select a cell, use the cell list (Figure 4.8#5).

4. Cell layout displays the selected cell showing the number of lanes on the mainline and on the ramps if they are present. Auxiliary lanes are colored in gray.

5. Cell list is used to select a cell for editing.

6. Cell parameter panel displays editable parameters of the selected cell.

- **Length** – cell length in *miles*.
- **Lanes** – number of lanes.
- **Auxiliary Lanes** – number of auxiliary lanes.
- **Maximum Flow** – cell capacity per lane, measured in *vehicles per hour per lane* (vphl).
- **Critical Density** – critical density, measured in *vehicles per mile per lane* (vpml).
- **Jam Density** – jam density, measured in *vehicles per mile per lane* (vpml).
- $\mathbf{V_f}$ – free flow speed, measured in *miles per hour* (mph).
- $\mathbf{W_c}$ – congestion wave speed, measured in *miles per hour* (mph).
- **On-Ramp** checkbox indicates the presence (when checked) of an on-ramp in the cell. If the on-ramp is present, then the on-ramp parameter panel is displayed (Figure 4.8#8), otherwise it is hidden.

- **Off-Ramp** checkbox indicates the presence (when checked) of an off-ramp in the cell. If the off-ramp is present, then the off-ramp parameter panel is displayed (Figure 4.8#9), otherwise it is hidden.

7. **Fundamental diagram** plot displays the fundamental diagram. The values of capacity, critical density and jam density are given *per lane*.
8. **On-ramp parameter** panel is displayed if the **On-Ramp** checkbox in the cell parameter panel is checked (Figure 4.8#6). It contains the on-ramp parameters.

- **Name** – string containing the on-ramp name. It must be nonempty.
- **Lanes** – number of lanes.
- **Maximum Flow** – on-ramp capacity per lane, measured in *vehicles per hour per lane* (vphl).
- **Queue Size** – queue limit. This parameter is used only by queue controllers.
- **Gamma** – on-ramp flow blending coefficient. It must be in the range between [0,1].
- $\mathbf{X_i}$ – on-ramp flow allocation parameter. It must be in the range between 0 and 1.

9. Off-ramp parameter panel is displayed if the **Off-Ramp** checkbox in the cell parameter panel is checked (Figure 4.8#6). It contains the off-ramp parameters.

- **Name** – string containing the off-ramp name. It must be nonempty.
- **Lanes** – number of lanes.
- **Maximum Flow** – off-ramp capacity per lane, measured in *vehicles per hour per lane* (vphl).
- **Split Ratio** – off-ramp split ratio, a portion of vehicles directed to the off-ramp from the mainline. It must be in the range between 0 and 1.

10. **Add Cell button** – if clicked, adds a new cell with default parameters immediately downstream of the selected cell.

11. **Duplicate Cell button** – if clicked, adds a clone of the selected cell immediately downstream of it.

12. **Delete Cell button** – if clicked, removes the selected cell.

b. CTMSIM Simulator.

To start the CTMSIM Simulator with given configuration file myconfig.mat in graphical mode, type

>> ctmsim myconfig

Figure 4.10(a) presents the look of the CTMSim Simulator. The application window is partitioned into 9 areas.

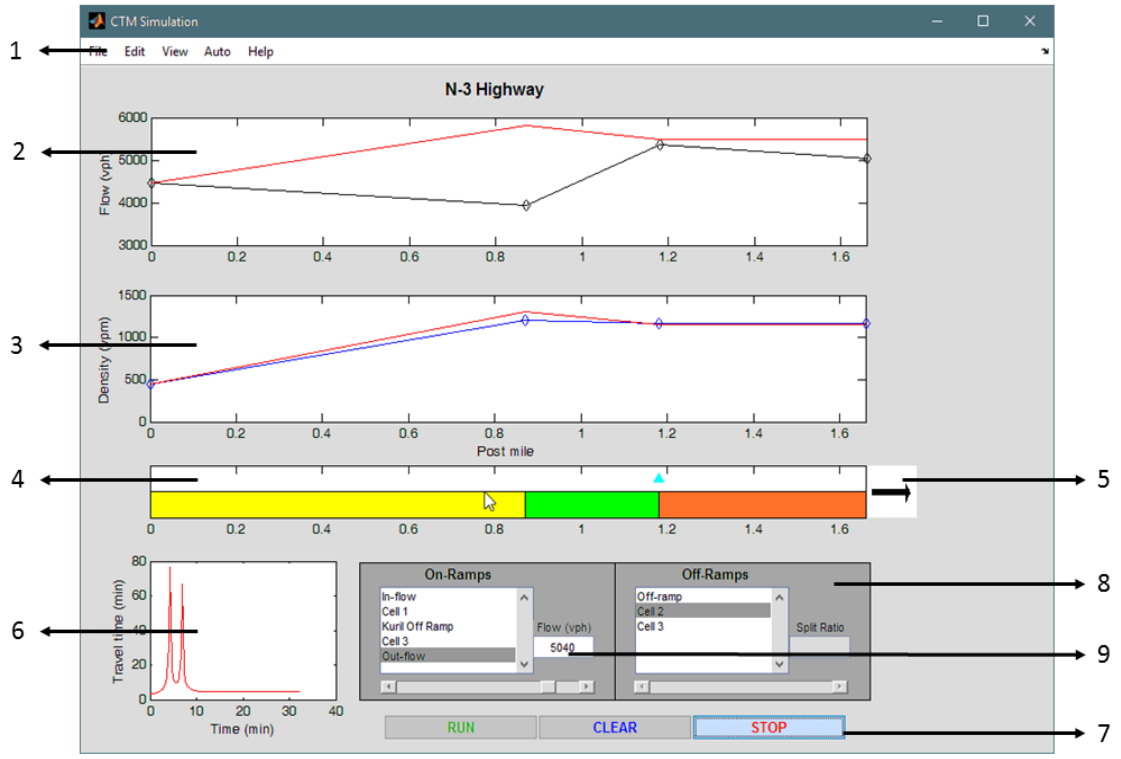

(a)

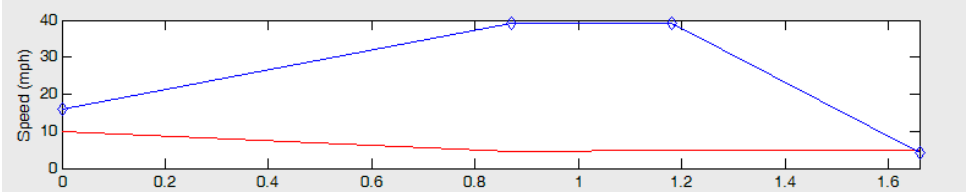

(b)

Figure 4.10 CTMSim Simulator.

1. Menu bar.

2. First data plotting area. Figure 4.10(a) shows flows (back) and the capacities (red) plotted per cell.

3. Second data plotting area. Figure 4.10(a) shows densities (blue) and the critical densities (red) plotted per cell. Instead of densities, the user may choose to plot speeds (blue) and free flow speeds (red) as in Figure 410(b). Instead of flows and densities/speeds, the first and second data plotting areas can display the following data plots.

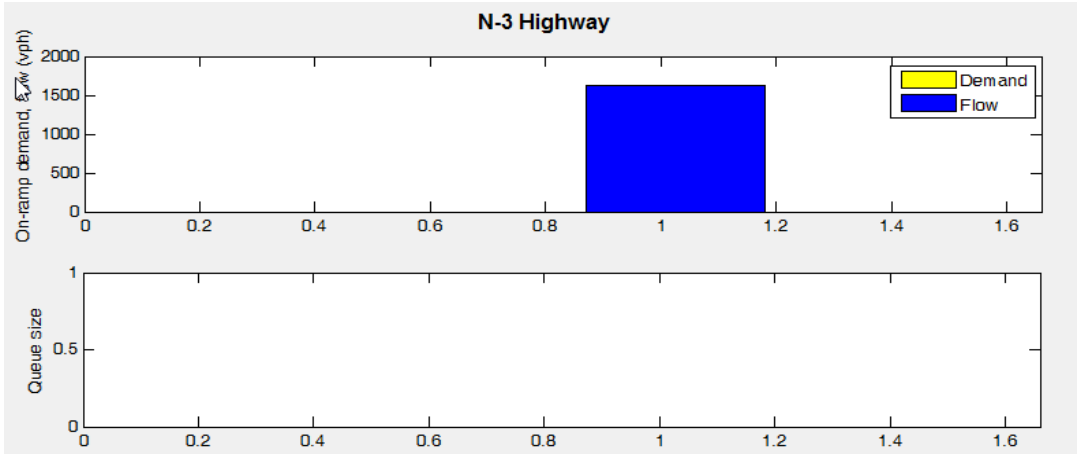

(a)

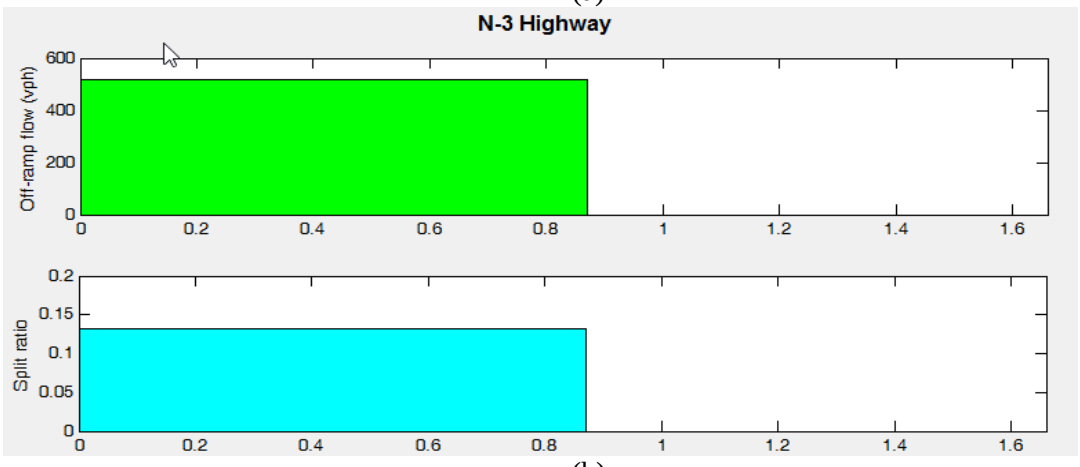

(b)

Figure 4.11 Data displayed in the Simulator window.

- On-ramp demands, flows and queue sizes (menu option View → On-Ramp Demands and Queues, Figure 4.11a). Demand values are shown as yellow bars, and flows – as blue bars in each cell. If a user sees only a blue bar in some cell, it means

that on-ramp flow equals the demand. If, on the other hand, only the yellow bar is visible, it means that on-ramp flow is zero. Otherwise, the user should see both yellow and blue bars. If the yellow bar is higher than the blue, this indicates that either some control is turned on at this on-ramp, or that the demand exceeds ramp capacity, in which case the queue starts to grow. The situation when the blue bar is higher than the yellow is only possible if there exists a queue at the on-ramp, and the ramp can let through more vehicles than the demand, resulting in decreasing queue size.

- Off-ramp flows and split ratios (menu option View → Off-Ramp Flows and Split Ratios, Figure 4.11b). Split ratios are either constant (the user can change them manually as simulation runs), or taken from the split ratio profile (configuration variable betaProfile, see Appendix A) – in this case the off-ramp flows are computed in the simulation. Alternatively, off-ramp flows can be taken from the offramp profile (configuration variable frflowProfile, see Appendix A), in which case the split ratios are computed in the simulation.

Instead of plotting selected quantities only at the current simulation step, the user may choose to see the history of how the system evolved in time by looking at time contours (menu option View → Timeseries Contours). Figure 4.13 shows an example of flow and speed time contours.

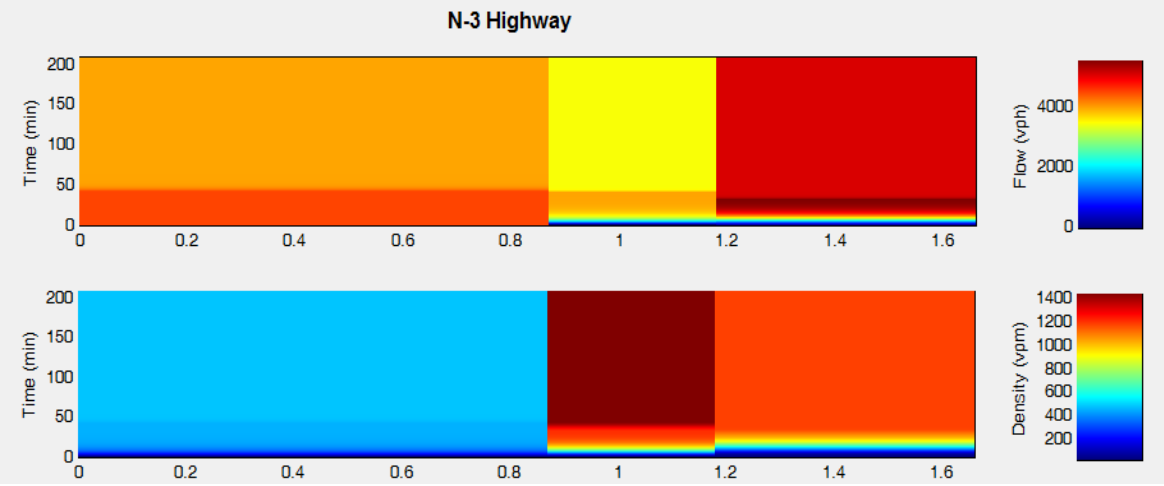

4. Freeway layout shows how the simulated freeway segment is divided into cells whose sizes on the screen are proportional to their lengths. Corresponding post miles are at the bottom of the plot. During the simulation the color coding is used to display the status of each cell: green means free flow, red means congested. There are two auxiliary colors: yellow indicates free flow at 97% of capacity, orange indicates congested flow at 97% of capacity. The threshold 97% is a configurable parameter (configuration variable yoColorRatio, see Appendix A). The blue triangular marker shows which on-ramp is currently selected from the list of on-ramps. An on-ramp is always at the beginning of the cell. The cyan triangular marker shows which off-ramp is currently selected from the list of off-ramps. An off-ramp is always at the end of the cell.

5. The arrow specifies the traffic orientation. Left-to-right corresponds to directions North and East, and right-to-left corresponds to directions South and West.

6. **Aggregate data plotting area** by default displays the plot of instantaneous travel time through the mainline of the simulated freeway segment.

7. **On-ramp panel** displays the list of on-ramps. This list contains all the cells, but only those with on-ramps have meaningful names, the other ones are named Cell #, where # denotes the cell number. The user can select an on-ramp from the list and manually change the flow. This makes sense only if the demand profile is not used, otherwise, all the values set by the user will be overwritten by the values from the demand profile and values computed by the Simulator. The selected on-ramp is marked by the blue triangle in the freeway layout (Figure 4.10(a)#4).

8. **Off-ramp panel** displays the list of off-ramps. This list contains all the cells, but only those with off-ramps have meaningful names, the other ones are named Cell #, where # denotes the cell number. The user can select an off-ramp from the list and

manually change the split ratio. This makes sense only if the split ratio and off-ramp flow profiles are not used, otherwise, all the values set by the user will be overwritten by the values from the split ratio profile or values computed by the Simulator. The selected off-ramp is marked by the cyan triangle in the freeway layout (Figure 4.10(a)#4).

9. **Simulation control panel** has three buttons.

- RUN button – starts the simulation or resumes it after it was paused.
- CLEAR button. If the simulation is paused, it resets the simulation to its initial state, otherwise (if the simulation is running), it continues the simulation execution treating current state and time as new initial conditions and discarding all previously computed simulation data.
- STOP button – pauses the simulation

4.4 Model Calibration for Non-Lane-Based Heterogeneous Traffic

The basic CTMSim is developed based on the basic FD of Triangular shape without any capacity lag. However, with time the analysis of FD reveals that the shape we considered earlier doesn't remain constant over time. Moreover, we estimated the characteristic parameters of a highway section from FD which makes the analysis of FD more important. CTM also evolves the traffic state as well as speed-flow-density from FD. From our extensive analysis on FD, we have already found in previous section (Section 4.2) that the non-linear behavior of FD for urban non-lane-based heterogeneous traffic. These non-linear equations of v-ρ have been considered instead of simple triangular FD in simulation stage and the computation of basic CTM has been changed in following way:

a. Compute initial and boundary conditions i.e. Cell length, time step size, initial density at 0 time step of the simulation, on- and off-ramp flows at 0 time step, inflow, upstream demand in the gate cell, downstream capacity etc.

b. Set time step k = 0.

c. Initialize on-ramp queue size $q_i(0)$ =0, i = 1...N.

d. Initialize on-ramp flow $r_i(0) = R_i$, i = 1...N.

In cells without on-ramps, R_i is assumed to be 0.

e. Compute on-ramp flows

$$r_i(k+1) = \min\left\{\begin{array}{l} d_i(k+1) + \dfrac{qu_i(k)}{\Delta t}, \\ \xi_i(\rho_j - \rho_i(k))\dfrac{\Delta x_i}{\Delta t}, \\ R_i, \\ \max\{C(r_i(k)), Q(r_i(k))\} \end{array}\right\}, i = 1...N \quad \text{---------- (4.31)}$$

Where, $C(r_i(k))$ denotes flow value suggested by on-ramp mainline controller

$Q(ri(k))$ denotes the flow value coming from on-ramp queue controller.

f. Update queue sizes.

$$qu_i(k+1) = \max\{qu_i(k) + (d_i(k+1) - r_i(k+1))\Delta t, o\}, i = 1...N \quad (4.32)$$

g. Compute shockwave from following equation of FD.

$$w = -2.486\times10^{-5}\rho^3 + 0.0084\rho^2 - 1.035\rho + 55.44 \quad \text{---------- (4.33)}$$

$$w = -1.029\times10^{-6}\rho^3 + 0.008467\rho^2 - 0.2379\rho + 27.69 \quad \text{---------- (4.34)}$$

$$w = -1.921\times10^{-6}\rho^3 + 0.001407\rho^2 - 0.3488\rho + 34.40 \quad \text{---------- (4.35)}$$

h. Compute cell-to-cell flows

$$q_i(k+1)=\min\left\{\begin{array}{l}\overline{\beta_i}v_i(\rho_i(k)+\gamma_i r_i(k+1)\frac{\Delta t}{\Delta x_i}),\\ w_{i+1}(\rho_{j(i+1)}(k)-(\rho_{i+1}(k)+\gamma_{i+1}r_{i+1}(k+1)\frac{\Delta t}{\Delta x_{i+1}})),\\ \frac{\overline{\beta_i}}{\beta_i}S_i,\\ Q_i\end{array}\right\}, i=1...N \quad \text{---------- (4.36)}$$

i. Compute off-ramp flows

$$s_i(k+1)=\frac{\overline{\beta_i}}{\beta_i}f_i(k+1), if\ \beta_i<1 \quad \text{---------- (4.37)}$$

$$s_i(k+1)=\min\left\{v_i(\rho_i(k)+\gamma_i r_i(k+1)\frac{\Delta t}{\Delta x_i}, S_i\right\}, if\ \beta_i=1 \quad \text{---------- (4.38)}$$

j. Compute densities

$$\rho_i(k+1)=\rho_i(k)+(q_{i-1}(k+1)+r_i(k+1)-q_i(k+1)-s_i(k+1))\frac{\Delta t}{\Delta x_i}, i=1...N \quad \text{---------- (4.39)}$$

k. Compute actual speeds

$$V_i(k+1)=\min\left\{v_i, \frac{f_i(k+1)+s_i(k+1)}{\rho_i(k+1)}\right\}, i=1...N \quad \text{---------- (4.29)}$$

l. Compute travel time

$$TT(k+1)=\sum_{i=1}^{N}\frac{\Delta x_i}{w_i(k+1)} \quad \text{---------- (4.40)}$$

m. Set k=k+1.

n. Go to step e.

4.5 Model Validation

In the words of Papageorgiou (1998), empirical validation remains the final criterion measuring the degree of accuracy, and hence the usefulness, of any macroscopic traffic flow model. Accordingly, the modelled FD parameter with boundary values are incorporated in the basic CTM to estimate traffic states over time and the results are compared with the set of measured traffic data collected on the 16th of April, 2015. Since the model need the description of traffic demand for each time step for the whole simulation period, and initial density at 0 time step, these data on link L1 and L5, the gate cell and the sink respectively, are always assumed to be the measured field values. So, the traffic states of only the intermediate links L2, L3 and L4 are estimated by the model. Also, the on-ramp demand and off-ramp outflow are also taking the measured field data. The traffic states at the initial time step are assumed to be the measured field values for all interim the links. But after the first step, they are estimated by the model algorithm. The resulting speed, flow and density profiles for the intermediate links over the full simulation period are shown in Figures 4.13 (a-c). This comparison also includes the simulation data for Linear-FD which was considered earlier in basic computational model. As performance measure of the model, MAE is considered which quantifies the error between estimated and measured traffic states for the individual links both for linear and non-linear cases. MAE is defined as:

$$MAE_i = \frac{\sum_{k=1}^{k=450} \left| (Estimated(v,\rho,q)_k - Measured(v,\rho,q)_k) \right|}{\sum_{k=1}^{k=450} Measured(v,\rho,q)_k} \quad \text{---------- (4.41)}$$

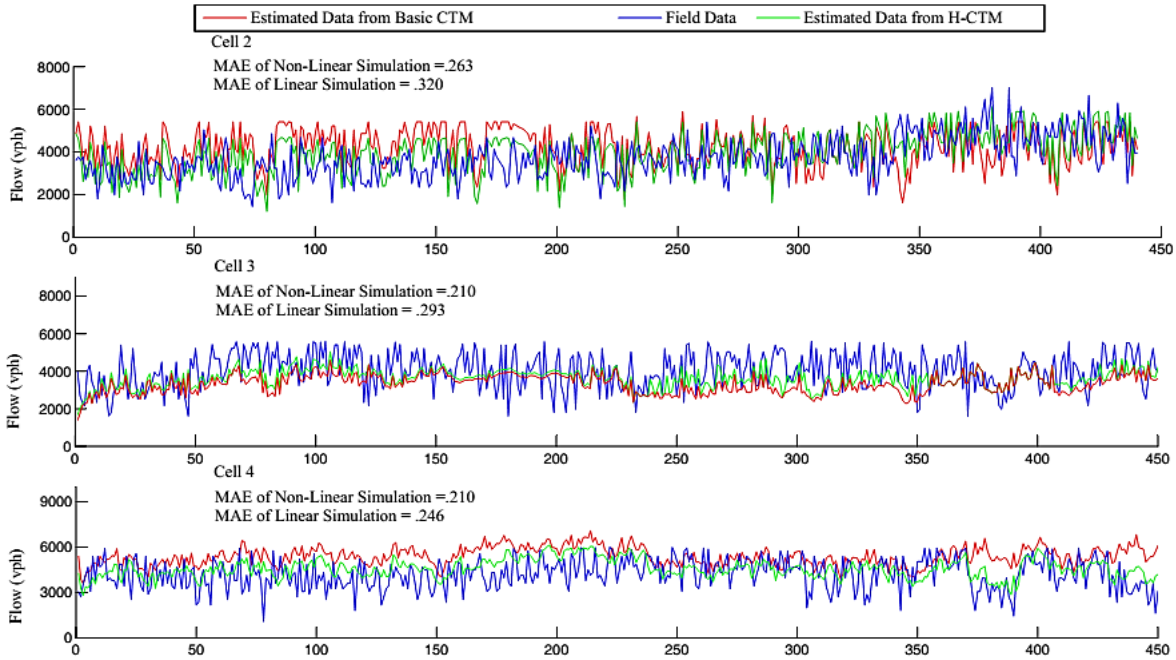

Figure 4.13 (a) Comparison between model estimated and field measured flow for different links.

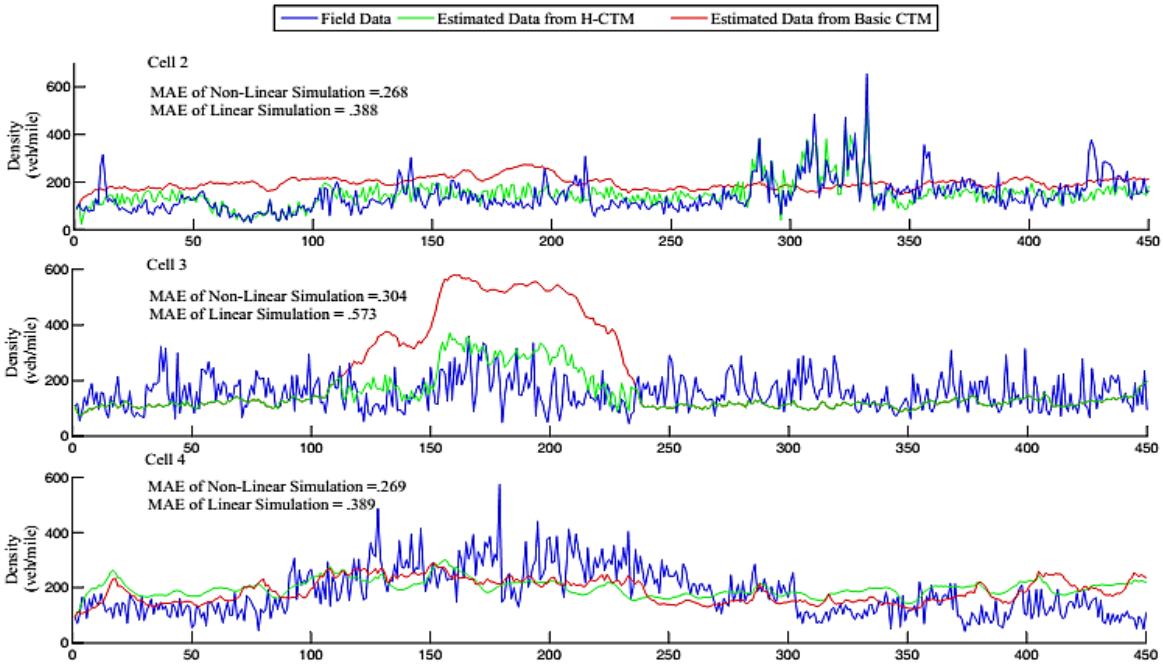

Figure 4.13 (b) Comparison between model estimated and field measured density data for different links.

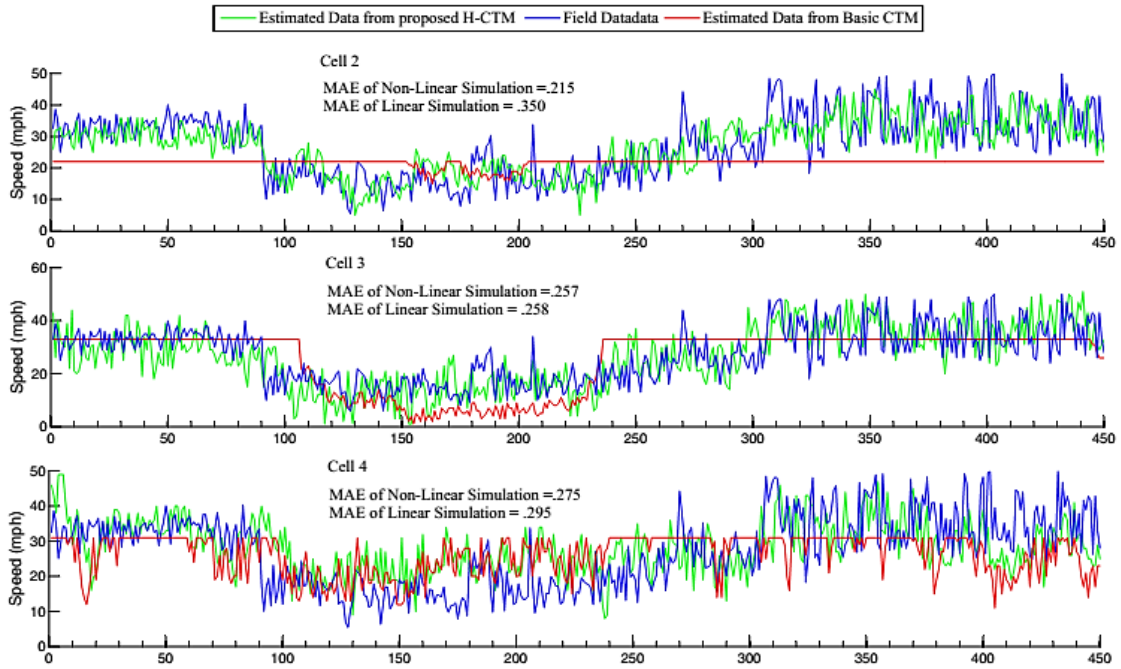

Figure 4.13 (c) Comparison between model estimated and field measured average speed data for different links.

From qualitative analysis of these figures, it is seen that the proposed model can estimate the field traffic states quite accurately and capture the traffic incident accurately. However, the flow data in link L2 shows poor performance than other two links. Nevertheless, compared to simulation data considering the linear FD, the result proves some improvement. This is due to the presence of an off-ramp in that link. We take the off-ramp flow data from field measurement and thus the simulation steps estimate the off-ramp split ration. Though the time step for our simulation is 20s, the change of split ration is more rapid and absence of continuity. This phenomenon is difficult for the model to capture even with the non-linear shockwave behaviour introduce in the model and results in a poor performance in that section. The inflow from the on-ramp in L3 causes the density to increase more rapidly in that link. The capacity of the 2-lane on-ramp was found 902 vphl which was hardly reached i.e. there was no queuing in the on-ramp and flow did not exceed the capacity of the ramp during our survey. In addition, there is no ramp controller installed that section. Therefore, only the flow-bending coefficient affects the flow equation (Equation 4.36) of the ramp.

We considered the flow blending coefficient γ_i as 1, which reflects that the position of on-ramp is at the beginning of the cell. Again, the flow allocation factor ξ_i is also considered as 1. This factor also influence the allocation of vehicle in available space; hence influence the on-ramp flow. These considerations are made due to the measurement shortcomings of our traffic survey. Nevertheless, this coefficient influences the density of the whole link from the beginning to the end. On the contrary, this increasing density does not affect the speed as well as flow behaviour of the section as the shockwave Equations 4.33, 4.34, 4.35 were modelled considering the density of the link itself which also includes the number of vehicles coming from the ramp. As the flow is estimated using the shockwave speed as well as the density considering from both the link and the ramp, the percentage of error reduces. The speed is showing good performance in L2, L3 and L4 as the shockwave speed is modelled beforehand. Though the linear FD considerations also shows good result in speed estimation, it cannot capture the speed profile accurately. In this regards, Non-linear FD consideration shows good performance.

TABLE 4.4 Sensitivity of the proposed model with respect to original model

Change in Model Structure	Link	MAE		
		v	q	ρ
Proposed CTM with Non-Linear FD	L2	.215	.263	.268
	L3	.257	.210	.304
	L4	.275	.210	.269
Basic CTM with Triangular FD	L2	.350	.320	.388
	L3	.258	.293	.573
	L4	.295	.246	.389

From Table 4.4, it is observed that the proposed model can simulate the measures traffic state with an accuracy of 72.5-78.5% for speed, 77.37-79% for flow and 69.6-73.2% for density estimation. Such accuracy can be considered quite satisfactory given the wide variations in operating and performance characteristics of non-lane-based

heterogeneous traffic while the original model shows poor performance than this model. From thorough investigation, we have found that these improvements in traffic flow simulation accuracy was achieved through incorporation of different factors in the original model. These factors include:

(1) Incorporation of non-linear FD (speed-density) model in CTM.

(2) Consideration of fixed free flow speed as boundary condition derived from non-linear FD

(3) New computational algorithm that influence flow and density estimation.

4.6 Chapter Summary

The current chapter focused on the development of a CTM with the incorporation of modelled non-linear FD for non-lane-based heterogeneous urban traffic condition in Dhaka City. For this, at first the nature of the fundamental traffic relationships were systematically investigated based on the traffic data collected earlier. From regression analysis it was concluded that 3rd degree polynomial structure shows the best fit with the measured traffic data. Moreover, careful observation of the operating and performance characteristics of heterogeneous traffic revealed that classical CTM tend to simulate inappropriate flow and speed behaviour due to simple and linear consideration of FD. The model proposed in this research was developed taking these findings into account. Next, based on the field data, all relevant model parameters were estimated in model calibration, using a modified algorithm from basic computational method. Then the calibrated model was used to successfully simulate traffic operations on the studied highway in the model validation stage. Finally, through investigation shows that the non-linear FD plays the most important role in CTM for estimating traffic state accurately in heterogeneous traffic operating condition.

CHAPTER 5

CONCLUSION AND RECOMMENDATION

6.1 Conclusion

This research develops a modified macroscopic first-order CTM that can simulate the heterogeneous traffic in non-lane-based traffic condition. The core of this model is FD, from which the dynamic model parameters are generated e.g. free-flow speed, shockwave, flow and density. The model is calibrated and validated for uninterrupted arterial with on- and off-ramp ramp in some cells. From sensitivity analysis, the simulation performance is found satisfactory enough to establish the model. It is expected that the model can reproduce same real time traffic state in other road classes of same nature. Main conclusion from this research are summarized chapter-wise below:

Chapter 2 provides elaborate state-of-the-art of traffic flow modelling, which includes the chronologic development of traffic flow models. Different criterion like *the scale of independent variables*, *the nature of variables*, *operationalization criterion and scale of application* etc. are selected for categorizing these models. Especially the CTM and application of macroscopic model in heterogeneous traffic state, are given emphasize. From extensive review, it has been found that; very small amount of study were undertaken for modelling heterogeneous traffic with CTM. In some cases, the researchers tried to incorporate class-wise and lane wise speed distribution in CTM, but it doesn't actually represent the system prevails in real. Because the system consists not only of car or bus but also other different class of vehicle. With these considerations the research is motivated to develop modified CTM for heterogeneous traffic.

Chapter 3 mainly focuses on the high-resolution data collection and processing techniques adopted in this research. It presents the geometric and traffic characteristics of the study site along with the details of the discretization process and the high-resolution traffic data collection method. Then a brief discussion on image processing technique used in this research for extracting flow and speed data from the video footages of the test site is included. The measured high-resolution data is used for the development and analysis of the macroscopic model in the subsequent chapters.

Chapter 4 is the most important part of the thesis. In this chapter the development, calibration and validation of the modified CTM along with the visual representation of simulation module is included. The main findings of the chapter are as following:

a) For developing of the model, at first step computation of the basic CTM with ordinary, diverging and merging link of cells is analysed. The basic model was proposed with trapezoidal FD, followed by triangular FD which is piecewise linear.

b) Then the FDs were modelled based on the field data obtained from chapter 3. The shockwave equations were generated as characteristic equation of FD, hence from the equation; free-flow speed, capacity, critical density, jam density is calculated. These values are used to calibrate the CTM parameters.

c) The user interface for visual feeling of the simulation is developed afterword, which is consists of two different windows: one stands for developing layout of geometric layout of the test site along with FD, another one gives the user a feeling of visual simulation. Brief description of both interfaces are also included in the chapter.

d) The modeled shockwave equations are incorporated in the modified CTM algorithm, fed into the user interface. CTM initiate simulation with its boundary condition and calibrated parameters. Then the link specific shockwave equation

estimate average speed from density and subsequently flow and other macroscopic parameters from CTM equations.

e) The results from the modified CTM are then compared with the actual field data. MAE for modified CTM is found within 30% (Table 4.4) for average speed, flow and density, while for basic CTM, MAE are found considerably higher based on the field data. The reason behind the MAE for non-linear FD considerations are also summarized in the chapter.

6.2 Future Scope of Work

Although traffic flow models have been studied for more than half a century in the developed world, research on this topic in Bangladesh as well as in other south-east Asian countries is extremely scarce and challenging. This is mainly due to the complexity of data collection and processing and the wide variations of driver population, vehicle components and traffic environment. Even though the current study tried to focus some effort in this sector, it cannot be viewed as a complete understanding of the highly complex heterogeneous traffic operation. In fact, it should be kept in mind that there is not a single traffic model that applies to all traffic situations. Further research to explore other forms of the traffic flow models for better representation of the heterogeneous traffic state evolution and traffic control is desirable in both theoretical analysis and field applications. In this section some recommendations are provided for future research following the studies carried out in this dissertation.

- The modified CTM has been developed from field data of specific time. If high-resolution data consisting all variations like, environmental, day-night, rush hour serge etc. can be collected, more realistic and accurate model can be developed.

- The modified CTM developed in this research is based on the uninterrupted freeway where homogeneous traffic condition prevails. However, this methodology of calibration has not yet been tested in interrupted freeway or urban signalized intersection.
- The model can also be tested for variable cell size to capture heterogeneous traffic more accurately.
- There is huge research scope of implementing this methodology in traffic control strategy where the same traffic condition reign.
- Moreover, this methodology can also be tested in ATDM, so that the city planners can have an actual and if necessary, dynamic representation of traffic state very quickly and accurately.
- As this model can capture traffic incident more accurately compared to the original, this methodology can be used in accident analysis i.e. impact on accident or any other moving bottleneck in the traffic stream.
- As our test site was a freeway arterial, Non Motorized Vehicle (NMV) was not considered. But in context of Bangladesh, NMV gives a considerable share to total urban traffic. So modelling FD considering NMV and calibrate CTM with it will also make a great contribution for countries like Bangladesh.

REFERENCE

1. Mahmud, S.S., M. Hoque, and G. Bashir. Deficiencies of Existing Road Network in Dhaka Metropolitan City. in *Publication in 10th Pacific Regional Science Conference Organization (PRSCO) Summer Institute*. 2008.
2. A. M. Khan and M.A. Mahmud, Transport Planning of Dhaka City: Some Contemporary Observations. *The Jahangirnagar University Planning Review*, 2013. **11**.
3. Daganzo, C.F., The cell transmission model: A dynamic representation of highway traffic consistent with the hydrodynamic theory. *Transportation Research Part B: Methodological*, 1994. **28**(4): p. 269-287.
4. Lighthill, M.J. and G.B. Whitham. On kinematic waves. II. A theory of traffic flow on long crowded roads. in *Proceedings of the Royal Society of London A: Mathematical, Physical and Engineering Sciences*. 1955. The Royal Society.
5. Greenberg, H., An analysis of traffic flow. *Operations research*, 1959. **7**(1): p. 79-85.
6. Greenshields, B., W. Channing, and H. Miller. A study of traffic capacity. in *Highway research board proceedings*. 1935. National Research Council (USA), Highway Research Board.
7. Tuerprasert, K. and C. Aswakul, Multiclass cell transmission model for heterogeneous mobility in general topology of road network. *Journal of Intelligent Transportation Systems*, 2010. **14**(2): p. 68-82.
8. Wardrop, J.G., Road paper. Some theoretical aspects of road traffic research. *Proceedings of the institution of civil engineers*, 1952. **1**(3): p. 325-362.
9. Gardels, K., Automatic car controls for electric highways. *General Motors Research Laboratories: GMR-276. Warren Michigan, June*, 1960.

10. Manual-HCM, H.C., Transportation Research Board. *National Research*, 2010.
11. Pipes, L.A., An operational analysis of traffic dynamics. *Journal of applied physics*, 1953. **24**(3): p. 274-281.
12. Brackstone, M. and M. McDonald, Car-following: a historical review. *Transportation Research Part F: Traffic Psychology and Behaviour*, 1999. **2**(4): p. 181-196.
13. Wilson, R.E. and J.A. Ward, Car-following models: fifty years of linear stability analysis–a mathematical perspective. *Transportation Planning and Technology*, 2011. **34**(1): p. 3-18.
14. Gipps, P.G., A behavioural car-following model for computer simulation. *Transportation Research Part B: Methodological*, 1981. **15**(2): p. 105-111.
15. Leutzbach, W., Introduction to the theory of traffic flow. Vol. 47. 1988: Springer.
16. Chandler, R.E., R. Herman, and E.W. Montroll, Traffic dynamics: studies in car following. *Operations research*, 1958. **6**(2): p. 165-184.
17. Newell, G.F., INSTABILITY IN DENSE HIGHWAY TRAFFIC: A REVIEW. 1965.
18. Gazis, D.C., R. Herman, and R.W. Rothery, Nonlinear follow-the-leader models of traffic flow. *Operations research*, 1961. **9**(4): p. 545-567.
19. Bando, M., et al., Analysis of optimal velocity model with explicit delay. *Physical Review E*, 1998. **58**(5): p. 5429.
20. Treiber, M., A. Kesting, and D. Helbing, Three-phase traffic theory and two-phase models with a fundamental diagram in the light of empirical stylized facts. *Transportation Research Part B: Methodological*, 2010. **44**(8): p. 983-1000.

21. Kerner, B.S. and S.L. Klenov, A microscopic model for phase transitions in traffic flow. *Journal of Physics A: Mathematical and General*, 2002. **35**(3): p. L31.

22. Kerner, B.S. and S.L. Klenov, Deterministic microscopic three-phase traffic flow models. *Journal of Physics A: mathematical and general*, 2006. **39**(8): p. 1775.

23. Michaels, R. Perceptual factors in car following. in *Proceedings of the 2nd International Symposium on the Theory of Road Traffic Flow (London, England), OECD*. 1963.

24. Wiedemann, R., Simulation des Strassenverkehrsflusses. 1974.

25. Lee, J.J. and J. Jones, Traffic dynamics: visual angle car following models. *Traffic Engineering & Control*, 1900. **8**(8).

26. Evans, L. and R. Rothery, Perceptual Thresholds in Car-Following-A Comparison of Recent Measurements with Earlier Results. *Transportation Science*, 1977. **11**(1): p. 60-72.

27. Krauß, S., K. Nagel, and P. Wagner. The Mechanism of Flow Breakdown in Traffic Flow Models. in *Transportation and Traffic Theory: Papers Presented at the Abbreviated Presentation Sessions*. 1999.

28. Cassidy, M.J. and R.L. Bertini, Observations at a freeway bottleneck. *Transportation and Traffic Theory*, 1999: p. 107-146.

29. Moridpour, S., M. Sarvi, and G. Rose, Lane changing models: a critical review. *Transportation letters*, 2013.

30. Sukthankar, R., S. Baluja, and J. Hancock. Evolving an intelligent vehicle for tactical reasoning in traffic. in *Robotics and Automation, 1997. Proceedings., 1997 IEEE International Conference on*. 1997. IEEE.

31. Alexiadis, V., D. Gettman, and R. Hranac, *Next Generation Simulation (NGSIM): Identification and Prioritization of Core Algorithm Categories*. 2004, Department ofTransportation Federal HighWay Administration (FHWA).

32. Halkias, B., et al., Freeway bottleneck simulation, implementation, and evaluation. *Transportation Research Record: Journal of the Transportation Research Board*, 2008.

33. Gartner, N.H., C.J. Messer, and A.K. Rathi, Traffic flow theory: A state-of-the-art report. 2001: Committe on Traffic Flow Theory and Characteristics (AHB45).

34. Richards, P.I., Shock waves on the highway. *Operations research*, 1956. **4**(1): p. 42-51.

35. LeVeque, R.J. and R.J. Leveque, Numerical methods for conservation laws. Vol. 132. 1992: Springer.

36. Gazis, D.C., Mathematical Theory of Automobile Traffic: Improved understanding and control of traffic flow has become a fast-growing area of scientific research. *Science (New York, NY)*, 1967. **157**(3786): p. 273-281.

37. Daganzo, C.F., The cell transmission model, part II: network traffic. *Transportation Research Part B: Methodological*, 1995. **29**(2): p. 79-93.

38. Gomes, G. and R. Horowitz, Optimal freeway ramp metering using the asymmetric cell transmission model. *Transportation Research Part C: Emerging Technologies*, 2006. **14**(4): p. 244-262.

39. Muñoz, L., et al. Traffic density estimation with the cell transmission model. in *American Control Conference, 2003. Proceedings of the 2003*. 2003. IEEE.

40. Daganzo, C.F., The lagged cell-transmission model. 1999.

41. Szeto, W., Enhanced lagged cell-transmission model for dynamic traffic assignment. *Transportation Research Record: Journal of the Transportation Research Board*, 2008(2085): p. 76-85.

42. Xiaojian, H., W. Wei, and H. Sheng, Urban traffic flow prediction with variable cell transmission model. *Journal of Transportation Systems Engineering and Information Technology*, 2010. **10**(4): p. 73-78.

43. Lee, S., *A cell transmission based assignment-simulation model for integrated freeway/surface street systems*. 1996, The Ohio State University.

44. Chen, X., Q. Shi, and L. Li, Location specific cell transmission model for freeway traffic. *Tsinghua Science & Technology*, 2010. **15**(4): p. 475-480.

45. Long, J., et al., Urban traffic jam simulation based on the cell transmission model. *Networks and Spatial Economics*, 2011. **11**(1): p. 43-64.

46. Tiriolo, M., L. Adacher, and E. Cipriani, An urban traffic flow model to capture complex flow interactions among lane groups for signalized intersections. *Procedia-Social and Behavioral Sciences*, 2014. **111**: p. 839-848.

47. Wang, P., *Conditional cell transmission model for two-way arterials in oversaturated conditions*. 2010, The University of Alabama TUSCALOOSA.

48. Huang, K.C., *Traffic Simulation Model for Urban Networks: CTM-URBAN*. 2011, Concordia University.

49. Skabardonis, A. and N. Geroliminis, *Real-time estimation of travel times on signalized arterials*. 2005.

50. Feldman, O. and M. Maher. Optimisation of traffic signals using a cell transmission model. in *34th Annual Universities' Transport Study Group Conference, Napier University, Edinburgh*. 2002. Citeseer.

51. Lo, H.K., A cell-based traffic control formulation: strategies and benefits of dynamic timing plans. *Transportation Science*, 2001. **35**(2): p. 148-164.

52. Almasri, E. and B. Friedrich, Online offset optimisation in urban networks based on cell transmission model. *ITS Hanover*, 2005.

53. Lin, W.-H. and D. Ahanotu, Validating the basic cell transmission model on a single freeway link. *PATH technical note; 95-3*, 1995.

54. Muñoz, L., et al., Piecewise-linearized cell transmission model and parameter calibration methodology. *Transportation Research Record: Journal of the Transportation Research Board*, 2006(1965): p. 183-191.

55. Sumalee, A., et al., Stochastic cell transmission model (SCTM): a stochastic dynamic traffic model for traffic state surveillance and assignment. *Transportation Research Part B: Methodological*, 2011. **45**(3): p. 507-533.

56. Alecsandru, C.D., *A stochastic mesoscopic cell-transmission model for operational analysis of large-scale transportation networks*. 2006, Louisiana State University.

57. Kimms, A. and K.-C. Maassen, Optimization and simulation of traffic flows in the case of evacuating urban areas. *OR spectrum*, 2011. **33**(3): p. 571-593.

58. Kimms, A. and K.-C. Maassen, Extended cell-transmission-based evacuation planning in urban areas. *Pesquisa Operacional*, 2011. **31**(3): p. 405-441.

59. Lo, H. A dynamic traffic assignment formulation that encapsulates the cell-transmission model. in *14th International Symposium on Transportation and Traffic Theory*. 1999.

60. Hadiuzzaman, M., T.Z. Qiu, and Y. Lin. Real-time Traffic State Estimation and Prediction for Active Traffic and Demand Management: The Application of

DynaTAM. in *CICTP 2012: Multimodal Transportation Systems—Convenient, Safe, Cost-Effective, Efficient*. 2012. ASCE.

61. Hadiuzzaman, M. and T.Z. Qiu, Cell transmission model based variable speed limit control for freeways. *Canadian Journal of Civil Engineering*, 2013. **40**(1): p. 46-56.

62. Alvarez-Icaza, L. and G.J. Islas. Hysteretic cell transmission model. in *16th International IEEE Conference on Intelligent Transportation Systems (ITSC 2013)*. 2013. IEEE.

63. Zhang, H.M., A theory of nonequilibrium traffic flow. *Transportation Research Part B: Methodological*, 1998. **32**(7): p. 485-498.

64. Payne, H.J., Models of freeway traffic and control. *Mathematical models of public systems*, 1971.

65. Payne, H.J., FREFLO: A macroscopic simulation model of freeway traffic. *Transportation Research Record*, 1979(722).

66. Papageorgiou, M., J.-M. Blosseville, and H. Hadj-Salem, Modelling and real-time control of traffic flow on the southern part of Boulevard Peripherique in Paris: Part I: Modelling. *Transportation Research Part A: General*, 1990. **24**(5): p. 345-359.

67. Lyrintzis, A.S., G. Liu, and P.G. Michalopoulos, Development and comparative evaluation of high-order traffic flow models. *Transportation Research Record*, 1994(1457).

68. Papageorgiou, M., Some remarks on macroscopic traffic flow modelling. *Transportation Research Part A: Policy and Practice*, 1998. **32**(5): p. 323-329.

69. Venkatesan, K., A. Gowri, and R. Sivanandan, Development of microscopic simulation model for heterogeneous traffic using object oriented approach. *Transportmetrica*, 2008. **4**(3): p. 227-247.

70. Arasan, V.T. and R.Z. Koshy, Methodology for modeling highly heterogeneous traffic flow. *Journal of Transportation Engineering*, 2005. **131**(7): p. 544-551.

71. Jin, S., et al., Non-lane-based full velocity difference car following model. *Physica A: Statistical Mechanics and Its Applications*, 2010. **389**(21): p. 4654-4662.

72. Gunay, B., Car following theory with lateral discomfort. *Transportation Research Part B: Methodological*, 2007. **41**(7): p. 722-735.

73. Raghava Chari, S. and K. Badarinath, Study of mixed traffic stream parameters through time lapse photography. *Highway Research Bulletin,(New Delhi)*, 1983(20): p. 57-83.

74. Gupta, A. and S. Khanna. Mixed traffic flow analysis for developing countries WST to India. in *Research for Tomorrow's Transport Requirements. Proceedings of the Fourth World Conference on Transport Research*. 1986.

75. Nair, R., H.S. Mahmassani, and E. Miller-Hooks, A porous flow approach to modeling heterogeneous traffic in disordered systems. *Transportation Research Part B: Methodological*, 2011. **45**(9): p. 1331-1345.

76. Tuerprasert, K. and C. Aswakul. An extension of cell transmission model for heterogeneous mobility. in *15th World Congress on Intelligent Transport Systems and ITS America's 2008 Annual Meeting*. 2008.

77. https://its.mit.edu/software/mitsimlab/technical-information.

78. Ngoduy, D., Multiclass first-order traffic model using stochastic fundamental diagrams. *Transportmetrica*, 2011. **7**(2): p. 111-125.

79. Liu, H., et al., Integrating the Bus Vehicle Class Into the Cell Transmission Model. *IEEE Transactions on Intelligent Transportation Systems*, 2015. **16**(5): p. 2620-2630.

80. Wong, G. and S. Wong, A multi-class traffic flow model–an extension of LWR model with heterogeneous drivers. *Transportation Research Part A: Policy and Practice*, 2002. **36**(9): p. 827-841.

81. Muniruzzaman, S.M., et al., DETERMINISTIC ALGORITHM FOR TRAFFIC DETECTION IN FREE-FLOW AND CONGESTION USING VIDEO SENSOR.

82. Underwoo, R., Speed, volume and density relationships: quality and theory of traffic flow, Yale Bureau of Highway Traffic,(1961), 141-188. *New Haven, Connecticut*, 2008.

83. Edie, L.C., Car-following and steady-state theory for noncongested traffic. *Operations Research*, 1961. **9**(1): p. 66-76.